4228

J. Am. Chem. Soc. **1993,** *115,* 4228–4245

Structural and Thermodynamic Characterization of Temperature-Dependent Changes in the Folding Pattern of a Synthetic Triamide[†]

Gregory P. Dado and Samuel H. Gellman*

Contribution from the S. M. McElvain Laboratory of Organic Chemistry, Department of Chemistry, University of Wisconsin, 1101 University Avenue, Madison, Wisconsin 53706

Received April 6, 1992

Abstract: Variable-temperature ¹H NMR and IR studies of triamide 1 and related compounds indicate that 1 undergoes dramatic temperature-dependent conformational changes in relatively nonpolar solvents (methylene chloride and chloroform). The folding pattern favored at low temperatures in these chlorocarbons (1c) contains a single C=O···H—N hydrogen bond in a nine-membered ring, while a folding pattern containing only a six-membered-ring C=O···N—H interaction (1a) is favored at higher temperatures. Dimethyl sulfoxide, a very strong hydrogen-bond-accepting solvent, disrupts all internal hydrogen bonding in 1. Acetonitrile appears to disrupt the six-membered-ring hydrogen bond selectively and to promote nine-membered-ring interaction at room temperature, relative to chlorocarbon solvents. By treating the behavior of 1 as a two-state system, in which folding pattern 1c is considered to be the "native state" and all other folding patterns comprise the "denatured state", we have been able to carry out van't Hoff analyses of the temperature-dependent conformational changes. In methylene chloride, the native state is enthalpically preferred by 1.9–2.5 kcal/mol but entropically disfavored by 7.4–9.1 eu. Similar values are obtained in chloroform. This thermodynamic characterization demonstrates that, even in a relatively nonpolar environment, the relative enthalpic stabilities of alternative folding patterns cannot be predicted simply by maximizing the pairing of hydrogen-bond donors and acceptors.

Introduction

The proper functioning of molecules and molecular assemblies in biological systems often requires precise spatial orientation of components. This inter- and intramolecular order is generally achieved through networks of noncovalent interactions. Elucidating the manner in which such networks of individually weak interactions control conformation and complexation represents a continuing and fundamental challenge for chemists, with applications in drug design, protein engineering, and other important technologies. The characterization of noncovalently controlled structure in solution is a major source of difficulty in this area. Folding patterns and intermolecular complexes often have a dynamic nature on operationally important spectroscopic time scales that leads to ambiguities not usually encountered in the establishment of covalently controlled structure.

Conformational analysis of peptides in solution is an interesting example in this regard. Analysis of flexible linear peptides containing one to several tens of residues has often focused on attempts to define a single preferred conformation.[1] Even when the existence of multiple folding patterns has been taken into account and probed, such studies have seldom provided quantitative information on conformational populations.[2] Thermodynamic relationships among alternative peptide conformational states have rarely been characterized.[3] (The denaturation of many proteins has been characterized thermodynamically, but there is little structural information on the denatured state.[4])

We have been studying the folding of small natural and unnatural peptides in organic solvents in an effort to elucidate

the manner in which modest networks of noncovalent interactions control the adoption of compact molecular conformations.[5-8] Intramolecular dipolar attraction, including hydrogen bonding, is expected to be a principal driving force for folding in these systems. Folding may be opposed by steric and dipolar repulsions that develop as the molecules bend back upon themselves and by the loss of conformational entropy that accompanies the adoption of compact structures. Conformational equilibria in these systems should also be affected by differences in the interactions of solvent with alternative folding patterns. We have focused initially on molecules of low molecular weight because they offer the best opportunity for structural characterization of the folding patterns that are highly populated in solution. Studies of this type may be viewed as a prelude to efforts to dissect the network of noncovalent interactions that specifies the folding and complexation behavior of biopolymers.

We recently reported that triamide 1 in methylene chloride

† Dedicated to the memory of Professor Margaret C. Etter.

(1) (a) Rose, G. D.; Gierasch, L. M.; Smith, J. A. *Adv. Protein Chem.* **1985,** *37,* 1. (b) Considerable effort has been devoted to the study of small cyclic peptides because of their tendency to adopt well-defined conformations; for leading references, see: Kessler, H. *Angew. Chem., Int. Ed. Engl.* **1982,** *21,* 512.

(2) (a) Boussard, G.; Marraud, M. *J. Am. Chem. Soc.* **1985,** *107,* 1825. (b) Milburn, P. J.; Konishi, Y.; Meinwald, Y. C.; Scheraga, H. A. *J. Am. Chem. Soc.* **1987,** *109,* 4486. (c) Milburn, P. J.; Meinwald, Y. C.; Takahashi, S.; Ooi, T.; Scheraga, H. A. *Int. J. Pept. Protein Res.* **1988,** *31,* 311.
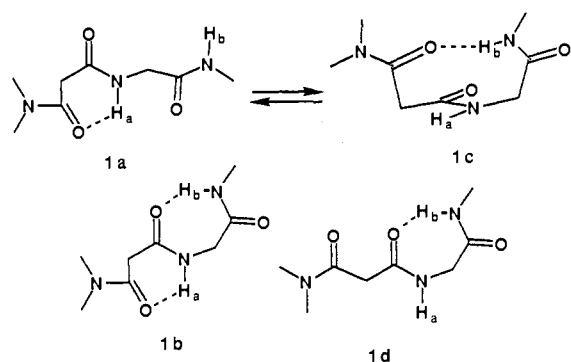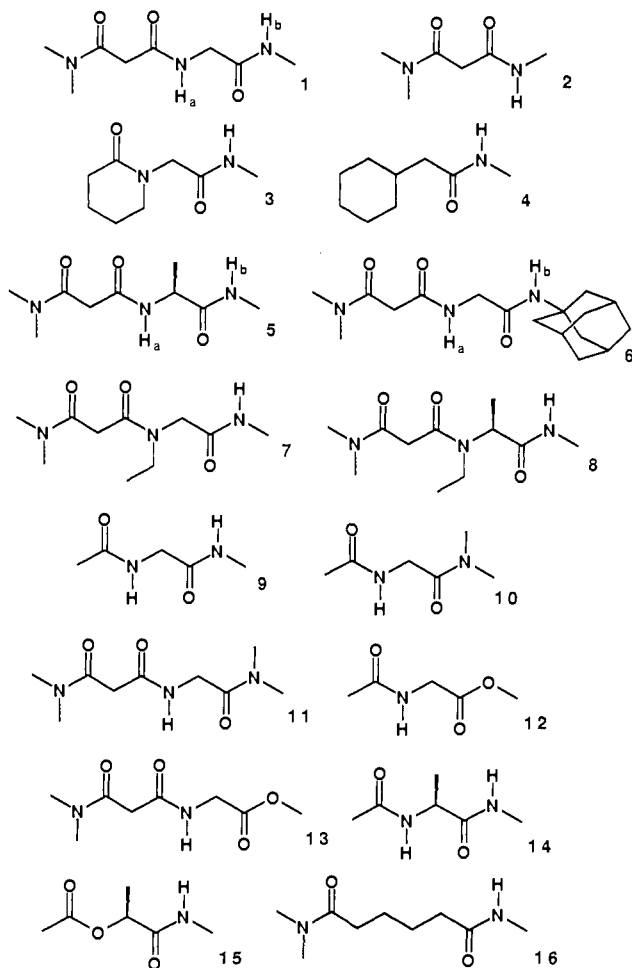
(3) For leading references on quantitative studies of α-helix vs coil equilibria of small peptides, see: (a) Scholtz, J. M.; Marqusee, S.; Baldwin, R. L.; York, E. J.; Stewart, J. M.; Santoro, M.; Bolen, D. W. *Proc. Natl. Acad. Sci. U.S.A.* **1991,** *88,* 2854. (b) O'Neil, K. T.; DeGrado, W. F. *Science* **1990,** *250,* 646. (c) Lyu, P. C.; Liff, M. I.; Marky, L. A.; Kallenbach, N. R. *Science* **1990,** *250,* 669. Very recent reports call into question the nature of the "folded state" in these peptide model systems: (d) Miick, S. M.; Martinez, G. V.; Fiori, W. R.; Todd, A. P.; Millhauser, G. L. *Nature* **1992,** *359,* 653. (e) Lovejoy, B.; Choe, S.; Cascio, D.; McRorie, D. K.; DeGrado, W. F.; Eisenberg, D. *Science* **1993,** *259,* 1288.

(4) For leading references, see: (a) Dill, K. A. *Biochemistry* **1990,** *31,* 7133. (b) *Prediction of Protein Structure and the Principles of Protein Conformation*; Fasman, G. D., Ed.; Plenum Press: New York, 1989. (c) Dill, K. A.; Shortle, D. *Annu. Rev. Biochem.* **1991,** *60,* 795.

(5) (a) Gellman, S. H.; Adams, B. R.; Dado, G. P. *J. Am. Chem. Soc.* **1990,** *112,* 460. (b) Dado, G. P.; Desper, J. M.; Gellman, S. H. *J. Am. Chem. Soc.* **1990,** *112,* 8630. (c) Dado, G. P.; Desper, J. M.; Holmgren, S. K.; Rito, C. J.; Gellman, S. H. *J. Am. Chem. Soc.* **1992,** *114,* 4834.

(6) (a) Liang, G.-B.; Rito, C. J.; Gellman, S. H. *Biopolymers* **1992,** *32,* 293. (b) Liang, G.-B.; Rito, C. J.; Gellman, S. H. *J. Am. Chem. Soc.* **1992,** *114,* 4440.

(7) Gellman, S. H.; Dado, G. P.; Liang, G.-B.; Adams, B. R. *J. Am. Chem. Soc.* **1991,** *113,* 1164.

(8) Liang, G.-B.; Dado, G. P.; Gellman, S. H. *J. Am. Chem. Soc.* **1991,** *113,* 3994.

Scheme I

Chart I

Figure 1. Amide proton NMR chemical shifts of 1–3 and N-methylacetamide, 1 mM in CD_2Cl_2, as a function of temperature. H_a of triamide 1 (●); H_b of triamide 1 (▲); diamide 2 (□); diamide 3 (△); N-methylacetamide (○).

Figure 2. Comparison of amide proton NMR chemical shifts of 1 in CD_2Cl_2, as a function of temperature, obtained at 5.0 and 1.0 mM and linearly extrapolated to 0 amide concentration on the basis of measurements at 5.0, 1.0, and 0.5 mM. H_a of triamide 1, 5 mM (+); H_b of triamide 1, 5 mM (×); H_a of triamide 1, 1 mM (●); H_b of triamide 1, 1 mM (▲); H_a of triamide 1, extrapolated to 0 concentration (○); H_b of triamide 1, extrapolated to 0 concentration (△).

Our goals have been (i) to identify the folding patterns adopted by triamide 1 at various temperatures in methylene chloride, (ii) to quantify the folding thermodynamics in this solvent, and (iii) to examine the effects of other solvents on the intramolecular hydrogen-bonding equilibrium. For these last studies, we have employed chloroform (a solvent of similarly low polarity to methylene chloride), acetonitrile (which is moderately polar), and dimethyl sulfoxide (which is very polar).

Results

Variable-Temperature ^1H NMR Data in CD_2Cl_2. Figure 1 shows the temperature dependences of the amide proton NMR chemical shifts for 1 mM samples of 1–3 in CD_2Cl_2. (Structures for compounds 1–16 are shown in Chart I.) Also shown are the $\Delta\delta NH/\Delta T$ data for a 1 mM sample of N-methylacetamide. As discussed above, triamide 1 has several hydrogen-bonding options available to it. Diamide 2, on the other hand, can experience only a single intramolecular hydrogen bond, in a six-membered ring with a covalent connectivity identical to that of the six-membered-ring interaction available to 1. Diamide 3 also has

solution experiences striking changes in its intramolecular hydrogen-bonding pattern as a function of temperature.[5a] A folding pattern containing only a nine-membered-ring hydrogen bond (1c) is favored at low temperatures, and at higher temperatures a folding pattern containing a six-membered-ring hydrogen bond (1a) becomes increasingly populated (Scheme I). The folding pattern in which the largest number of hydrogen-bond donors and acceptors is paired (1b) does not appear to be significantly populated under any conditions, even though the solution environment is relatively nonpolar. The folding pattern containing only a seven-membered-ring hydrogen bond (1d) also does not appear to be significantly populated at any temperature. Our preliminary reports have elicited examinations of 1 and related compounds by molecular mechanics[9] and semiempirical[10] methods; these computational studies have produced predictions that are inconsistent with our experimental findings.

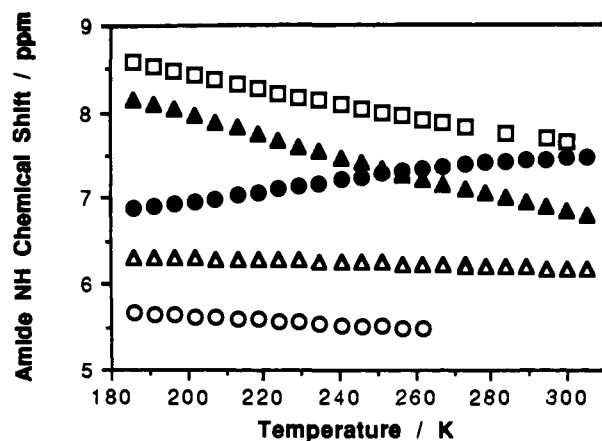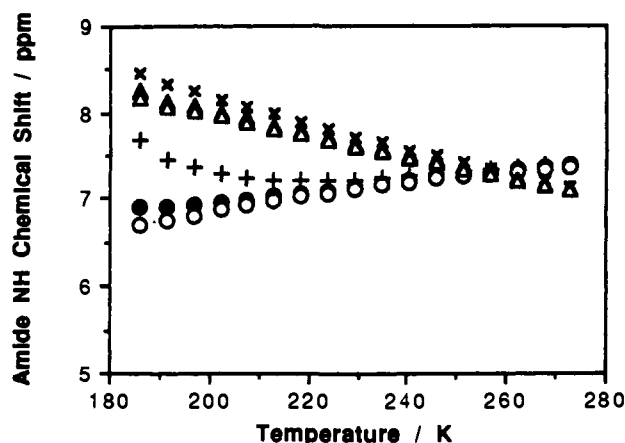We report here a thorough study of 1 and related compounds.

(9) (a) Smith, D. A.; Vijayakumar, S. *Tetrahedron Lett.* **1991**, *32*, 3613. (b) Smith, D. A.; Vijayakumar, S. *Tetrahedron Lett.* **1991**, *32*, 3617. (c) For a critical evaluation of these computational results, see: Gellman, S. H.; Dado, G. P. *Tetrahedron Lett.* **1991**, *32*, 7737. See also the Note Added in Proof.
(10) (a) Novoa, J. J.; Whangbo, M.-H. *J. Am. Chem. Soc.* **1991**, *113*, 9017. (b) For a discussion of these results, see: Dado, G. P.; Gellman, S. H. *J. Am. Chem. Soc.* **1992**, *114*, 3138.
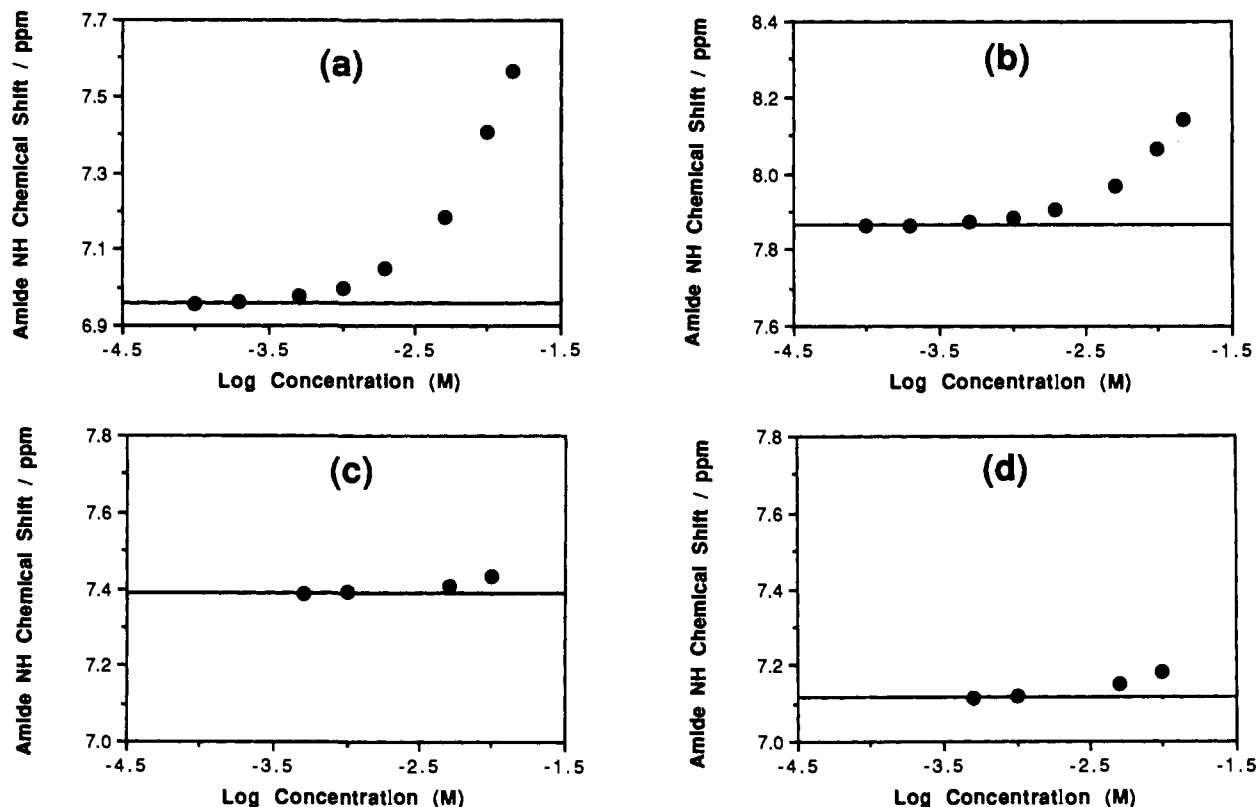
Figure 3. Amide proton NMR chemical shifts of triamide 1 in CD_2Cl_2 as a function of the logarithm of triamide concentration. (a) H_a at 208 K (0.01–15 mM); (b) H_b at 208 K (0.01–15 mM); (c) H_a at 273 K (0.5–5.0 mM); (d) H_b at 273 K (0.5–5.0 mM). In each case, the horizontal line represents the chemical shift value obtained by linear extrapolation to 0 concentration of data obtained at 5.0, 1.0, and 0.5 mM at that temperature.

only one possible intramolecular hydrogen bond, in a seven-membered ring that has the same covalent connectivity as the seven-membered-ring interaction available to 1.[11] The resonances of the two amide protons of 1 are resolved at nearly all temperatures. These resonances were assigned at low temperatures by their splitting patterns (H_a is a triplet and H_b is a quartet) and at high temperatures by homonuclear decoupling experiments. The $\Delta\delta NH/\Delta T$ signature for 1 mM *N*-methylacetamide represents the behavior of a secondary amide proton free of interaction with an amide carbonyl in CD_2Cl_2, because no IR absorption in the hydrogen-bonded N–H stretch region (3250–3400 cm^{-1}) can be detected in a 1 mM solution of *N*-methylacetamide in CH_2Cl_2 throughout this temperature range.

Comparison of the $\Delta\delta NH/\Delta T$ signatures for H_a and H_b of 1 with the data for 2 and 3 (Figure 1) indicates that the behavior of triamide 1 cannot be explained by invoking hydrogen bonding in only six- and seven-membered rings (states **1a**, **1b**, and **1d**). Two observations are particularly important in this regard. First, the resonance of H_b is quite far downfield at low temperatures. One cannot account for this downfield shift by invoking only a seven-membered-ring C=O⋯H—N hydrogen bond, because the amide proton resonance of 3 remains near 6.3 ppm throughout the temperature range. Second, the chemical shift of H_a moves downfield with increasing temperature. Amide protons involved in hydrogen bonds typically move upfield as the temperature is raised, which is conventionally interpreted to indicate a heat-

induced disruption of hydrogen bonding.[12] The unusual sense of the temperature dependence of H_a (Figure 1) suggests that this amide proton experiences an *increasing* amount of hydrogen bonding as the temperature is raised. (The interpretation of $\Delta\delta NH/\Delta T$ data will be discussed in greater detail below.)

In order to rule out the possibility that intermolecular interactions were responsible for the observations shown in Figure 1, we obtained variable-temperature ^{1}H NMR data for 1 at 5.0, 1.0, and 0.5 mM concentrations in CD_2Cl_2 and linearly extrapolated to 0 concentration. Figure 2 juxtaposes the $\Delta\delta NH/\Delta T$ signatures of H_a and H_b measured with 5 and 1 mM samples and the signatures obtained from the extrapolation to infinite dilution. The effects of aggregation are manifested in the downfield shifts of the 5 mM data; this comparison suggests that for the 1 mM sample there is, at most, a small amount of aggregation below 210 K and no significant aggregation above 210 K ($\geq$213 K, differences between the 1 mM data set and the extrapolation to infinite dilution are <0.05 ppm; $\geq$257 K, differences between the 5 mM data set and the extrapolation to infinite dilution are <0.05 ppm).

A referee has pointed out that a linear extrapolation to 0 concentration is not necessarily a rigorously correct way to account for aggregation, so we further characterized the effects of concentration on δH_a and δH_b of 1 at low temperature. Figures 3a and b show chemical shift data obtained at eight concentrations between 15 and 0.01 mM, 208 K, plotted as a function of the logarithm of triamide concentration. Figures 3c and d show data obtained at 273 K over the concentration range 5.0–0.5 mM plotted similarly. The horizontal lines in Figures 3a–d represent the chemical shift obtained by the linear extrapolation procedure described above. It is clear from these plots that the linear extrapolations provide an accurate estimate of δH_a and δH_b of 1 at infinite dilution over the entire temperature range. Therefore,

(11) Similar seven-membered ring hydrogen bonds are available to polypeptides constructed from α-amino acids. This hydrogen-bonded ring has been designated the C_7 or γ-turn conformation and has been the subject of considerable experimental and theoretical investigation. For leading references, see: (a) Böhm, H.-J.; Brode, S. *J. Am. Chem. Soc.* **1991**, *113*, 7129. (b) Perczel, A.; Angyan, J.; Kajtar, M.; Viviani, W.; Rivail, J.-L.; Marcoccia, J.-F.; Csizmadia, I. G. *J. Am. Chem. Soc.* **1991**, *113*, 6256. (c) Head-Gordon, T.; Head-Gordon, M.; Frisch, M. J.; Brooks, C. L.; Pople, J. A. *J. Am. Chem. Soc.* **1991**, *113*, 5989. (d) Roterman, I. K.; Lambert, M. H.; Gibson, K. D.; Scheraga, H. A. *J. Biomol. Struct. Dynam.* **1989**, *7*, 421. (e) Maxfield, F. R.; Leach, S. J.; Stimson, E. R.; Powers, S. P.; Scheraga, H. A. *Biopolymers* **1979**, *18*, 2507.

(12) (a) Kopple, K. D.; Ohnishi, M.; Go, A. *J. Am. Chem. Soc.* **1969**, *91*, 4264. (b) Ohnishi, M.; Urry, D. W. *Biochem. Biophys. Res. Commun.* **1969**, *36*, 194. (c) Stevens, E. S.; Sugawara, N.; Bonora, G. M.; Toniolo, C. *J. Am. Chem. Soc.* **1980**, *102*, 7048.
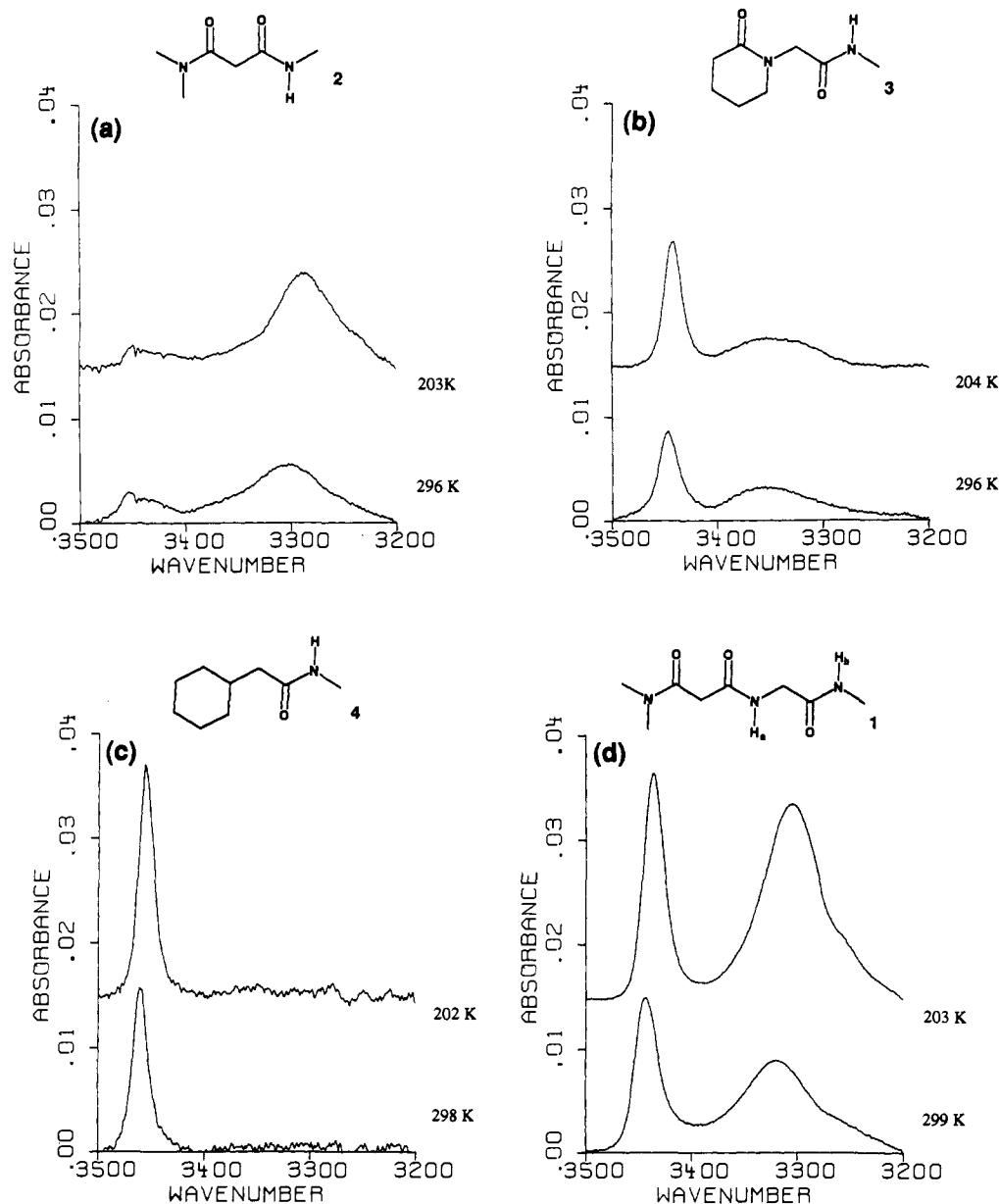
Figure 4. N–H stretch region FT-IR spectral data for 1 mM amide samples in CH_2Cl_2, after subtraction of the spectrum of pure CH_2Cl_2 at the same temperature. (a) Diamide 2 at 296 (absorption maxima at 3453, ca. 3435, and 3303 cm^{-1}) and 203 K (absorption maxima at 3449, ca. 3425, and 3288 cm^{-1}); (b) diamide 3 at 296 (absorption maxima at 3447 and ca. 3352 cm^{-1}) and 204 K (absorption maxima at 3442 and ca. 3343 cm^{-1}); (c) amide 4 at 298 (absorption maximum at 3460 cm^{-1}) and 202 K (absorption maximum at 3456 cm^{-1}); (d) triamide 1 at 299 (absorption maxima at 3443 and 3319 cm^{-1}) and 203 K (absorption maxima at 3436 and 3304 cm^{-1}).

we conclude that the temperature-dependent behavior of 1 at 1 mM in methylene chloride must be explained by invoking only intramolecular interactions.[13]

We can account for the data shown in Figure 1 by hypothesizing that folding pattern 1c is favored at low temperatures in methylene chloride and that 1a becomes increasingly populated as the temperature is raised. At most only minor amounts (<10%) of states containing the seven-membered ring interaction (i.e., 1b and 1d) and of states lacking any intramolecular hydrogen bond are present at any temperature, according to our model.

Variable-Temperature IR Data in CH_2Cl_2. Figure 4a shows the N–H stretch region of the IR spectrum of diamide 2, 1 mM in CH_2Cl_2, at 296 and 203 K. The broad absorption at ca. 3300 cm^{-1} may be assigned to N–H serving as a donor in a typical amide–amide hydrogen bond, and the small absorption at 3454 cm^{-1} may be assigned to a fully solvated N–H *in* CH_2Cl_2. We will refer below to this latter type of N–H moiety as "non-hydrogen-bonded", although there is presumably a weak interaction with the solvent.[7] The origin of the small absorption at ca. 3430 cm^{-1} in Figure 4a is not clear; this band could result

from a weak intramolecular hydrogen bond (e.g., to the π electron system of the dimethylamide moiety). The spectra in Figure 4a

(13) The referee has also suggested that the species detected spectroscopically at room temperature (i.e., near the top of our temperature range) in a 1 mM methylene chloride solution of 1 might be a dimer or higher oligomer. Several lines of reasoning argue against this possibility. (i) Diamide 9 has two amide protons in an analogous juxtaposition to the two amide protons in 1. The N–H stretch region IR spectrum of 1 mM 9 in methylene chloride (Figure 11a) shows a strong band at 3446 cm^{-1} (solvent-exposed N–H) and a shoulder at 3417 cm^{-1} (C_5 conformation; for assignments, see: Avignon, M.; Huong, P. V.; Lascombe, J.; Marraud, M.; Néel, J. *Biopolymers* 1969, 8, 69. Burgess, A. W.; Scheraga, H. A. *Biopolymers* 1973, 12, 2177. Ref 11e.) There is no evidence of significant intermolecular hydrogen bonding under these conditions (no bands between 3200 and 3400 cm^{-1}). It would be very surprising if the addition of a single tertiary amide group (to form 1 from 9) could convert a completely monomeric system to a completely associated system. (ii) Stevens et al. have studied the aggregation of a number of small peptides in chloroform solution by vapor pressure osmometry (ref 12c); they conclude that at 5 mM, Boc-Ala-Ala-OMe and related molecules are less than 10% associated at room temperature. (iii) The association constants for hydrogen-bonded dimer formation of N-methylacetamide, caprolactam, and butyrolactam in chloroform at room temperature are all in the range 1–3 M^{-1}; see: Krikorian, S. E. *J. Phys. Chem.* 1982, 86, 1875.
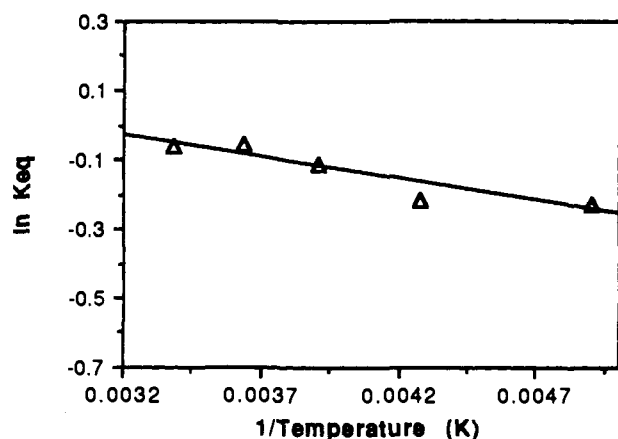
Figure 5. Representative van't Hoff plot constructed from N–H stretch region FT-IR data for 1 mM diamide 3 in CH_2Cl_2, 204–296 K, as described in the text. The line represents the best fit to the van't Hoff equation (ln $K_{eq} = -\Delta H°/RT + \Delta S°/R$), with $\Delta H° = +0.25$ kcal/mol and $\Delta S° = +0.75$ eu (correlation coefficient = 0.860). The ranges for the enthalpy and entropy values for non-hydrogen-bonded vs intramolecularly hydrogen-bonded 3 reported in the text are based on all combinations of three independent VT-IR data sets for 3 and seven independent VT-IR data sets for reference compound 4.

indicate that the molecule is predominantly intramolecularly hydrogen-bonded at both high and low temperatures, which is consistent with the implications of the $\Delta\delta NH/\Delta T$ data for 2 in Figure 1.

Figure 4b shows N–H stretch region IR data for a 1 mM solution of diamide 3 in CH_2Cl_2 at 296 and 204 K. At both temperatures, 3 shows a substantial population of solvent-exposed N–H moieties (absorption maxima 3442–3447 cm^{-1}), as well as some intramolecular hydrogen bonding (absorption maxima 3343–3352 cm^{-1}). We used IR data for 3 obtained at 204, 234, 256, 275, and 296 K to determine the enthalpic and entropic relationships between the non-hydrogen-bonded and intramolecularly hydrogen-bonded states. The IR spectrum of a 1 mM sample of N-methylcyclohexylacetamide (4) in CH_2Cl_2 (Figure 4c) shows only a single N–H stretch band, 3456–3460 cm^{-1}, between 202 and 298 K, indicating that no intermolecular amide–amide hydrogen bonding occurs under these conditions. Data for 4 allowed us to determine the integrated extinction of the non-hydrogen-bonded N–H stretch band as a function of temperature, and we used this information to estimate the concentration of non-hydrogen-bonded N–H in 1 mM samples of 3 at various temperatures. That portion of the total amide concentration not accounted for in this way was assumed to be intramolecularly hydrogen-bonded.[14] Figure 5 shows a representative van't Hoff plot. The results of replicate analyses indicate that the internally hydrogen-bonded state is 0.18–0.29 kcal/mol *less* enthalpically favorable than the state in which the N–H interacts only with solvent and that the internally hydrogen-bonded state is 0.3–1.1 eu more entropically favorable than the state lacking the internal hydrogen bond.[15,16] This thermodynamic profile has been discussed previously.[10b]

Adrian and Wilcox have reported that small quantities of water in $CDCl_3$ exert a profound effect on the van't Hoff enthalpy and entropy measured for hydrogen-bond-mediated recognition of 2-aminopyrimidine by receptors containing two carboxylic acid groups.[17] As we have previously reported,[7] our "dry" methylene

---

(14) Suitable reference compounds are not available for an independent determination of the integrated extinction coefficient of the hydrogen-bonded N–H stretch band, so quantification must be based exclusively on the non-hydrogen-bonded N–H stretch. We have previously shown that this type of IR-based van't Hoff analysis of intramolecular hydrogen bonding in flexible diamides provides quantitatively similar results to ^1H NMR-based van't Hoff analysis; see ref 7.

(15) Similar enthalpy and entropy values were calculated for intramolecular hydrogen bonding in 3 when the non-hydrogen-bonded N–H stretch band of N-methylacetamide was used as the reference compound instead of 4.
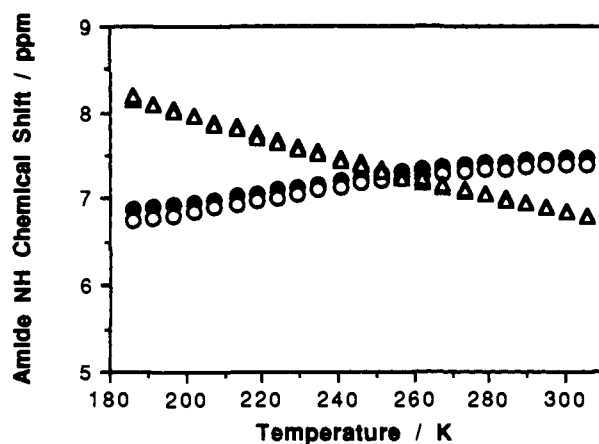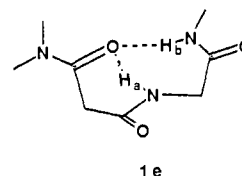
chloride samples contain 5–10 mM water in addition to the dissolved amide. We redetermined the IR-based van't Hoff enthalpy and entropy for intramolecularly hydrogen-bonded vs non-hydrogen-bonded 3 in the presence of ca. 15 and ca. 30 mM added D_2O and found no significant differences relative to $\Delta H°$ and $\Delta S°$ determined in dry CH_2Cl_2 (the details of these experiments may be found in the Experimental Section). Thus, trace amounts of water in our "dry" samples do not appear to influence the thermodynamic values we derive.

Figure 4d shows the N–H stretch region IR spectrum of triamide 1 at 299 and 203 K (1 mM in CH_2Cl_2). At both temperatures there are substantial populations of non-hydrogen-bonded and intramolecularly hydrogen-bonded N–H groups. The low-temperature spectrum rules out the possibility that doubly hydrogen-bonded state 1b or 1e is dominant at low temperature, if we assume that all C=O···H—N hydrogen bonds cause a $\Delta\bar{\nu}_{N-H}$ of >30 cm^{-1}. A qualitative comparison of the high- and low-temperature spectra for 1 suggests that the relative proportion of hydrogen-bonded and non-hydrogen-bonded N–H groups is similar at these two temperatures, which supports our hypothesis that the major effect of temperature on methylene chloride solutions of 1 is to alter the relative amounts of two folding patterns that each contain one hydrogen-bonded and one non-hydrogen-bonded N–H (1a and 1c).

Figure 6. Amide proton NMR chemical shifts of triamides 1 and 5, 1 mM in CD_2Cl_2, as a function of temperature. H_a of triamide 1 (●), H_b of triamide 1 (▲), H_a of triamide 5 (○), H_b of triamide 5 (△).

1 e

Steric Labeling of N–H Groups. Overlap of the hydrogen-bonded N–H stretch bands involving H_a and H_b and of the non-hydrogen-bonded N–H stretch bands involving H_a and H_b prevents a detailed analysis of the IR data for triamide 1 in Figure 4d. Previous work with small peptides suggested that it would be possible to achieve at least partial resolution of the narrow non-hydrogen-bonded N–H bands by altering the degree of alkyl substitution adjacent to the N–H moieties.[11c,18] We therefore examined triamide 5, in which the glycine residue of 1 is replaced with an alanine residue. Figure 6 juxtaposes the $\Delta\delta NH/\Delta T$ signatures for H_a and H_b of triamides 5 and 1, 1 mM each in CD_2Cl_2. The similarity between these data sets indicates that

---

(16) One potential source of systematic error in this type of study arises from the fact that the non-hydrogen-bonded N–H stretch band of 3 is not perfectly resolved from the hydrogen-bonded N–H stretch band. When a curve fitting procedure was employed to estimate the area of the isolated peak, qualitatively similar results were obtained.

(17) Adrian, J. C.; Wilcox, C. S. *J. Am. Chem. Soc.* **1991**, *113*, 678.

(18) Boussard, G.; Marraud, M.; Aubry, A. *Biopolymers* **1979**, *18*, 1297.
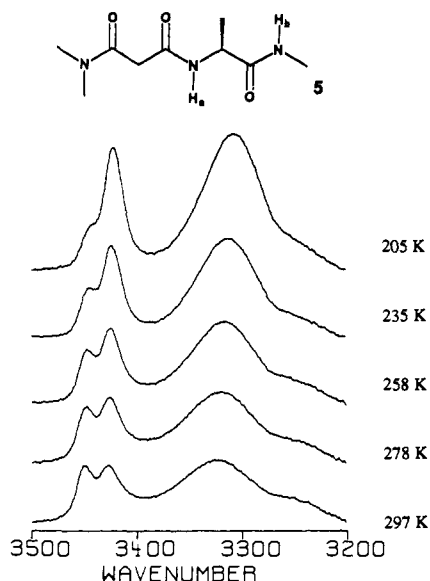
Figure 7. N–H stretch region FT-IR spectral data for 1 mM triamide **5** in CH_2Cl_2, after subtraction of the spectrum of pure CH_2Cl_2 at the same temperature.

the additional methyl group of **5** has little effect on the temperature-dependent changes in the triamide's folding pattern.

Figure 7 shows the N–H stretch region of the IR spectrum of 1 mM **5** in CH_2Cl_2 at several temperatures between 205 and 297 K. At the highest temperature, there are two substantial and partially resolved non-hydrogen-bonded N–H stretch bands, which were assigned by following H/D exchange of **5** in 0.2 M CD_3OD in $CDCl_3$ simultaneously via ^{1}H NMR and IR. This exchange process required several hours, and H_a exchanged significantly more rapidly than H_b. Correlation of the rates of H/D exchange in the ^{1}H NMR and IR spectra at room temperature showed that the band at 3427 cm^{-1} in Figure 7 (bottom trace) results from the non-hydrogen-bonded N–H_a stretch and that the band at 3449 cm^{-1} results from the non-hydrogen-bonded N–H_b stretch. These results are consistent with precedent.[11c,18]

If we assume that the extinction coefficients for non-hydrogen-bonded N–H_a and N–H_b stretch bands are similar to one another (supported by our observation that the extinction coefficient for N–H stretch bands of *N*-methylacetamide and *N*-isopropylacetamide are similar), then Figure 7 implies that at 297 K the non-hydrogen-bonded populations are similar for H_a and H_b. The non-hydrogen-bonded N–H_b band diminishes dramatically as the temperature is lowered and nearly disappears at 205 K, but the non-hydrogen-bonded N–H_a stretch band remains strong at this low temperature. This observation supports our hypothesis that only H_b serves as a hydrogen-bond donor in the folding pattern favored at low temperatures by the triamide skeleton that is common to **5** and **1**.

We also examined triamide **6** by IR, because the adamantyl substituent was expected to provide partial resolution of the non-hydrogen-bonded N–H_a and N–H_b stretch bands. In contrast to **5**, however, the band for N–H_a of **6** was expected to occur at higher wavenumber than the band for N–H_b. (We observed that a 1 mM solution of *N*-methylacetamide in CH_2Cl_2 showed a non-hydrogen-bonded N–H stretch band at 3460 cm^{-1} while a similar sample of *N*-1-adamantylacetamide showed a band at 3430 cm^{-1}.)

Figure 8 compares $\Delta\delta NH/\Delta T$ data for H_a and H_b of **6** in CD_2Cl_2 to analogous data for **1**. This comparison suggests that **6** undergoes a temperature-dependent change in folding pattern that is qualitatively similar to the change observed for **1**; however, the state of **6** containing the nine-membered-ring hydrogen bond appears to be less enthalpically favorable relative to the state containing the six-membered-ring hydrogen bond than **1c** is relative to **1a**. This conclusion derives from a comparison of the
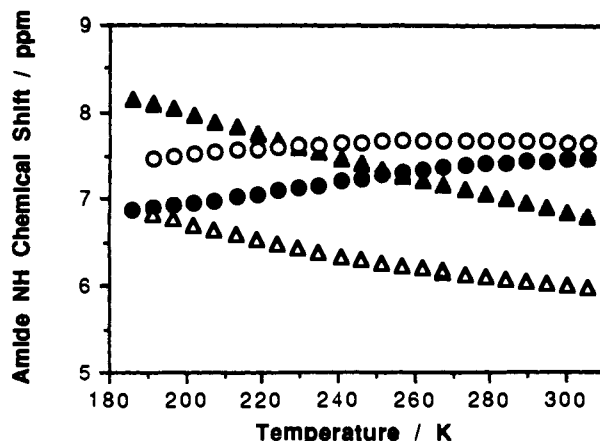

Figure 8. Amide proton NMR chemical shifts of triamides **1** and **6**, 1 mM in CD_2Cl_2, as a function of temperature. H_a of triamide **1** (●), H_b of triamide **1** (▲), H_a of triamide **6** (O), H_b of triamide **6** (△).
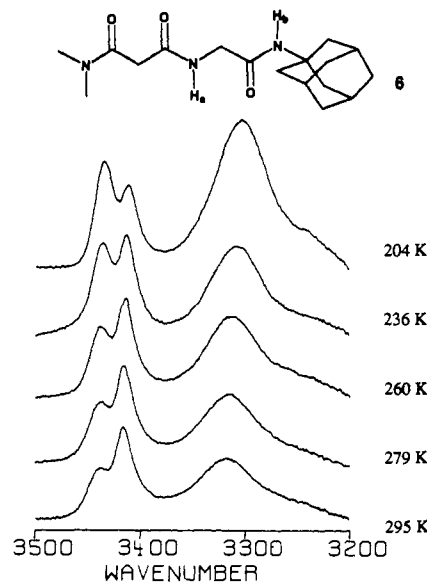

Figure 9. N–H stretch region FT-IR spectral data for 1 mM triamide **6** in CH_2Cl_2, after subtraction of the spectrum of pure CH_2Cl_2 at the same temperature.

$\Delta\delta NH/\Delta T$ signatures for H_a of **1** and **6**. Differences in δNH_a should largely reflect differences in the extent of internal hydrogen bonding experienced by these protons, since H_a should suffer relatively little change in chemical shift from the substitution of adamantyl for methyl. At all temperatures, δNH_a for **1** is smaller than δNH_a for **6**, and this consistent $\Delta\delta NH_a$ suggests that at each temperature there is more six-membered-ring hydrogen bonding in **6** than in **1**. Differences in δNH_b values throughout the temperature range are also consistent with the proposal that the nine-membered-ring hydrogen bond is less strongly enthalpically favored in **6** than in **1**.[19] (For *N*-1-adamantylacetamide, δNH is 0.3 ppm upfield of the corresponding δNH for *N*-methylacetamide; this $\Delta\delta NH$ value should provide a good estimate of $\Delta\delta NH_b$ for **6** vs **1**.)

Figure 9 shows the effect of temperature on the N–H stretch region IR spectrum of a 1 mM sample of triamide **6** in CH_2Cl_2. As expected, the non-hydrogen-bonded N–H_a and N–H_b stretch bands are partially resolved. Based on the lower non-hydrogen-bonded N–H stretch band position observed for *N*-1-adamantylacetamide relative to *N*-methylacetamide, we assigned the room temperature band at 3439 cm^{-1} to N–H_a and the band at 3416

(19) The origin of the difference between the folding of **1** and **6** is not clear. It is possible that the adamantyl methylene groups nearest to the carbon attached to the nitrogen sterically interfere with the approach of the hydrogen-bond acceptor; see ref 6b.
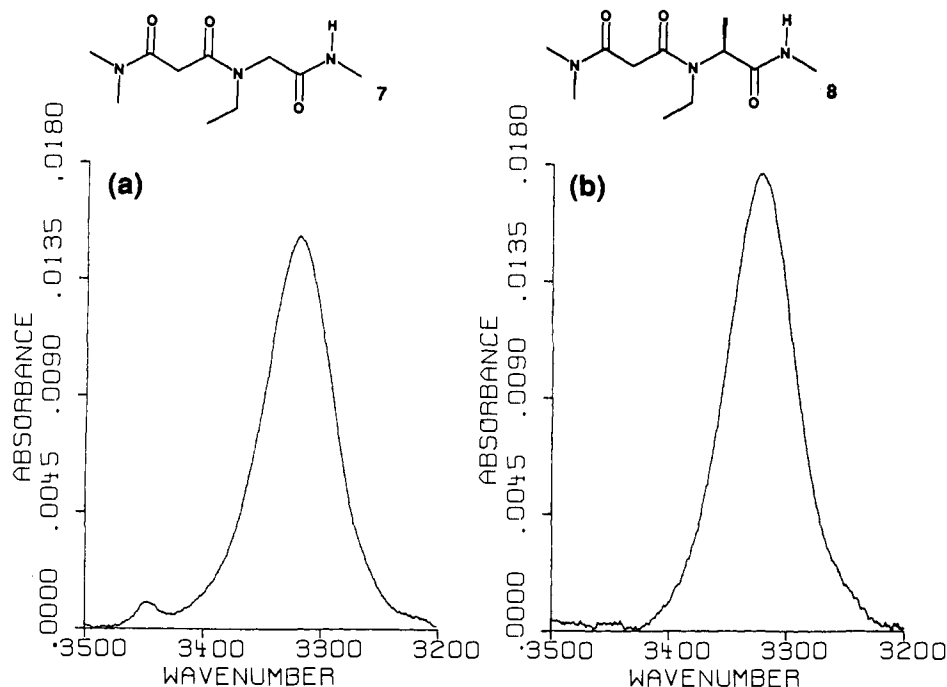
Figure 10. N–H stretch region FT-IR spectral data for 1 mM samples in CH_2Cl_2 at 298 K, after subtraction of the spectrum of pure CH_2Cl_2 at the same temperature. (a) Triamide 7 (absorption maxima at 3447 and 3320 cm^{-1}); (b) triamide 8 (absorption maximum at 3322 cm^{-1}).

cm^{-1} to N–H$_b$. The ratio of these bands' intensities changes as a function of temperature in a manner that is qualitatively consistent with our folding hypothesis for 1: the proportion of non-hydrogen-bonded N–H$_a$ relative to non-hydrogen-bonded N–H$_b$ increases at lower temperatures, as required if lower temperatures favor a folding pattern in which H$_b$ is involved in a nine-membered-ring interaction and H$_a$ is not engaged in an intramolecular hydrogen bond.

Replacement of H$_a$ with an Alkyl Group. Figure 10a shows the N–H stretch region IR spectrum of a 1 mM sample of triamide 7, in which H$_a$ of 1 is replaced by CH_2CH_3, and Figure 10b shows the spectrum for triamide 8, the analogous derivative of 5. The spectrum in Figure 10a indicates that the lone N–H group of 7 is almost completely internally hydrogen-bonded even at this relatively high temperature. Since diamide 3 experiences much less intramolecular hydrogen bonding under these conditions (Figure 4b), we conclude that the internal hydrogen bonding in 7 must involve a nine-membered-ring interaction rather than a seven-membered-ring interaction.[5a,8]

7a   7b
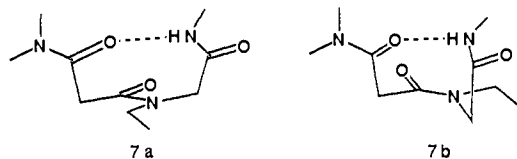
^{1}H NMR data indicated that two slowly interconverting forms of 7 were present in CD_2Cl_2 solution, in an approximately 13:1 ratio (not shown). We assigned these species as the (E) and (Z) rotamers about the central C–N bond on the basis of the observation that the ratio changed as a function of solvent (7:1 in CD_3CN, 2:1 in DMSO-d_6). Molecular models suggested that a nine-membered-ring hydrogen bond is possible in both the (Z) and (E) rotamers (7a and 7b, respectively). NOE experiments, summarized in Table I, identified the (Z) rotamer as the major species in CD_2Cl_2 solution. (Crystal structures have been determined for three triamides related to 7;[5b,c] all show the (Z) conformation about this C–N bond in the solid state, and two display the nine-membered-ring hydrogen bond.)

Smith and Vijayakumar have questioned the ability of NOE measurements to distinguish between the (Z) and (E) rotamers

Table I. NOE Data for Triamide 7

	NOEs observed (%)		
proton irradiated[a]	H$_a$ (δ 3.49)	H$_b$ (δ 3.96)	H$_c$ (δ 3.23)
H$_a$		<0.6	+2.5
H$_b$	<0.8		+1.7

[a] Experiments carried out in CD_2Cl_2 on the major solution rotamer; 2-s irradiation, 90° pulse.

of 7 about the central amide group's C–N bond in solution.[9b] These workers predicted that NOE enhancements would be observed among all three key methylene groups (malonyl, ethyl, and glycyl) in both the (Z) and (E) conformations. In order to address this question, we examined selected hydrogen–hydrogen distances in computationally minimized (AMBER/MacroModel v3.0[20]) structures of 7 containing a nine-membered-ring N—H···O=C hydrogen bond, with the central amide group in either the (Z) or (E) conformation (7a or 7b). For 7a, the shortest distance between hydrogen atoms on the malonyl and ethyl methylene groups was 2.28 Å, and the shortest distance between hydrogen atoms on the malonyl and glycyl methylene groups was 4.51 Å. For 7b, the shortest distance between hydrogen atoms on the malonyl and ethyl methylene groups was 4.66 Å, and the shortest distance between hydrogen atoms on the malonyl and glycyl methylene groups was 2.15 Å. Since the nuclear Overhauser effect is inversely proportional to the sixth power of the distance separating the hydrogen atoms involved, one expects a dramatic difference between such effects involving hydrogen atoms separated by 2.15–2.28 Å and hydrogen atoms separated by 4.51–

(20) AMBER: Weiner, S.; Kollman, P. A.; Nguyen, D. T.; Case, D. A. *J. Comput. Chem.* **1986**, *7*, 230. MacroModel: Mohamdi, F.; Richards, N. G. J.; Guida, W. C.; Liskamp, R.; Lipton, M.; Caufield, C.; Chang, C.; Chang, G.; Still, W. C. *J. Comput. Chem.* **1990**, *11*, 440.
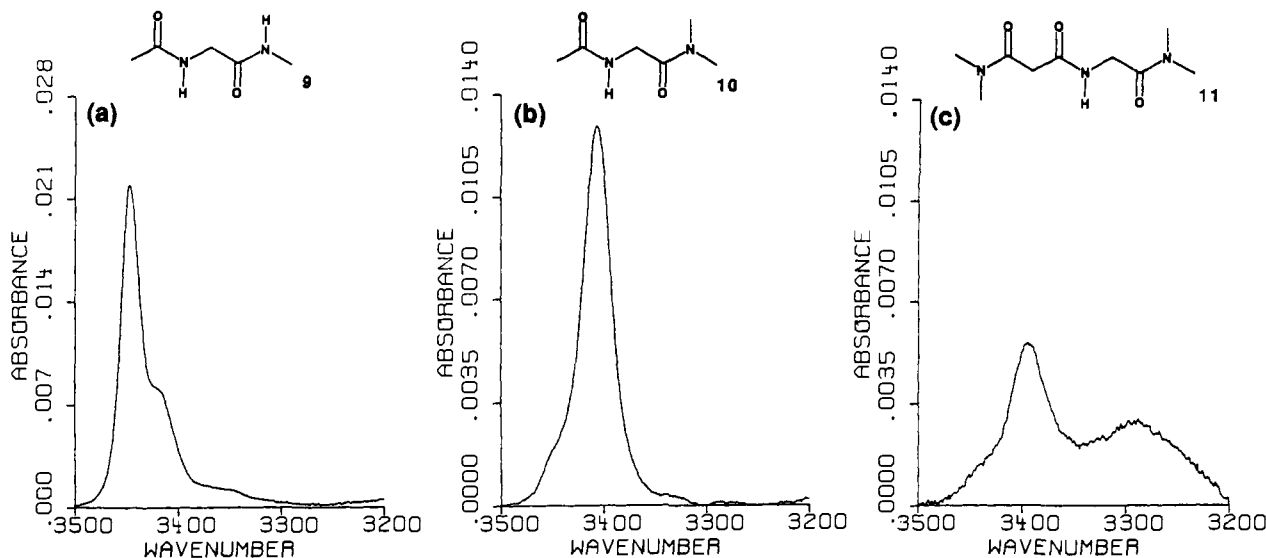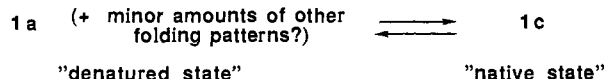
Figure 11. N–H stretch region FT-IR spectral data for 1 mM samples in CH_2Cl_2 at 297 K, after subtraction of the spectrum of pure CH_2Cl_2 at the same temperature. (a) Diamide **9** (absorption maxima at 3446 and 3417 cm⁻¹); (b) diamide **10** (absorption maximum at 3406 cm⁻¹); (c) triamide **11** (absorption maxima at 3394 and 3290 cm⁻¹).

Scheme II

4.66 Å. Therefore, Smith and Vijayakumar's concern about the use of NOE measurements to distinguish between **7a** and **7b** is unfounded.

Figure 10a shows that there is a small population of non-hydrogen-bonded N–H groups in a dilute CH_2Cl_2 solution of **7** at room temperature. It seems likely that these non-hydrogen-bonded N–H groups derive largely or exclusively from the minor (E) rotamer, because only this rotamer's amide proton chemical shift displayed a concentration dependence. At 293 K, the major rotamer's δNH in CD_2Cl_2 was invariant at 1, 10, and 100 mM, but the minor rotamer's δNH increased by 0.16 ppm between the 10 and 100 mM samples (the minor rotamer's N–H resonance could not be detected in the 1 mM sample).

Figure 10b shows that no non-hydrogen-bonded N–H stretch band can be detected for triamide **8** in dilute CH_2Cl_2, implying that both the (Z) and (E) rotamers about the central C–N bond of triamide **8** are completely intramolecularly hydrogen-bonded under these conditions. ^{1}H NMR data (1 mM) revealed a rotamer ratio of 3:1 for **8** in CD_2Cl_2. The $\Delta\delta$NH/ΔT signatures for both rotamers of **8** paralleled the $\Delta\delta$NH/ΔT signature for the major rotamer of **7** (all δNH values fell in the range 7.8–8.4 ppm from 190 to 300 K), which supports the hypothesis that both rotamers of **8** are fully intramolecularly hydrogen-bonded.

Thermodynamic Analysis of the Folding of Triamide 1. According to our conformational hypothesis, triamide **1** in dilute methylene chloride solution occurs largely in a highly ordered folded conformation (**1c**) at low temperatures (ca. 200 K) but prefers less ordered states (mostly **1a**, but possibly small amounts of completely non-hydrogen-bonded forms and other folding patterns) at higher temperatures. We define **1c** as the triamide's "native" state, and **1a** and any minor forms present at higher temperatures as the "denatured" state (Scheme II). In the context of this two-state model, eq 1 implies that the native state is enthalpically favored and that the denatured state is entropically favored. Further, the balance between the enthalpic advantage

$$\ln K_{eq} = -\Delta H^\circ/RT + \Delta S^\circ/R \qquad (1)$$

of the nine-membered-ring hydrogen-bonded state and the entropic advantage of the denatured state in this solvent must be

sufficiently fine that a significant variation of the relative populations can be observed over the accessible temperature range.

We used variable-temperature ^{1}H NMR data to determine the thermodynamic parameters for this two-state folding equilibrium. Because equilibration is rapid on the NMR time scale, the observed values for δH_a and δH_b of **1** at a given temperature are weighted averages of the chemical shifts of H_a and H_b in the limiting native and denatured states. Thermodynamic analysis of the data for H_b of **1** (Figure 1) requires that we account for $\Delta\delta NH_b/\Delta T$ in both of the limiting states.[7] Triamide **7** provides a good model for H_b in the native state at all temperatures, because, according to our hypothesis, H_b is fully engaged in a nine-membered-ring hydrogen bond in the native state. Furthermore, the folded form of **7** should reproduce the effects of all sources of magnetic anisotropy on H_b of **1a**. We examined two different molecules as models for H_b in the denatured state, **9** (N-acetylglycine methylamide) and diamide **3**. Figure 11a shows the IR spectrum of **9**. The lack of a band in the range 3300–3400 cm⁻¹ indicates that **9** experiences little or no seven-membered-ring hydrogen bonding under these conditions. Variations between **3** and **9** provide information on the difference between a secondary amide and a tertiary amide as the potential seven-membered-ring hydrogen-bond acceptor in **1**.

The choice of model compounds to represent $\Delta\delta NH_a/\Delta T$ in the native and denatured limiting states was less straightforward than for H_b. Compounds **10** and **11**, respectively, appear at first glance to be appropriate, but spectroscopic data reveal these compounds to be inadequate. Diamide **10** has been shown to experience a five-membered-ring interaction between the carbonyl oxygen and amide proton (the "C_5 conformation") in nonpolar solution.[21] Although the geometry of this N—H···O=C interaction is poor, IR data suggest that the interaction is indeed a weak hydrogen bond. Figure 11b shows the N–H stretch IR region of 1 mM **10** in CH_2Cl_2. The major band at 3406 cm⁻¹ is significantly lower than expected for a solvent-associated secondary amide N–H stretch but higher than expected for an N–H involved in a C=O···H—N hydrogen bond of good geometry.[7] Figure 11c shows that the C_5 conformation is also highly populated for triamide **11** in CH_2Cl_2 (strong band at 3394 cm⁻¹). In contrast, the folding pattern of triamide **1** containing only a C_5 interaction does not appear to be significantly populated at any temperature,

(21) Cung, M. T.; Marraud, J.; Néel, J. In *Proceedings of the 5th Jerusalem Symposium on Quantum Chemistry and Biochemistry*; Bergman, E., Pullman, B., Eds.; The Israel Academy of Sciences and Humanities: Jerusalem, 1973; p 69 and references therein.
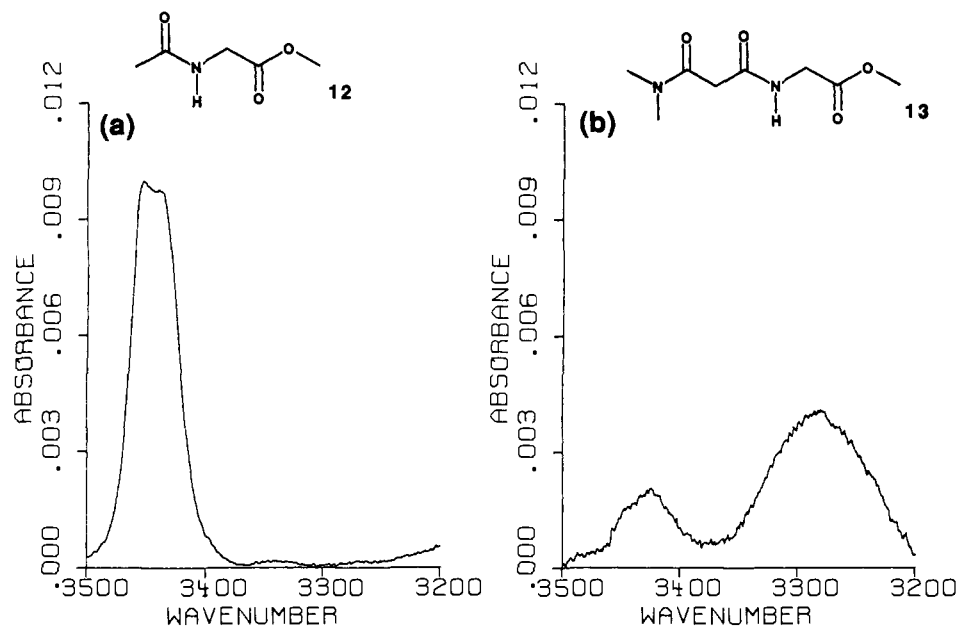
Figure 12. N–H stretch region FT-IR spectral data for 1 mM samples in CH_2Cl_2 at 297 K, after subtraction of the spectrum of pure CH_2Cl_2 at the same temperature. (a) Amide ester **12** (absorption maxima at 3452 and 3438 cm^{-1}); (b) diamide ester **13** (absorption maxima at 3424 and 3282 cm^{-1}).
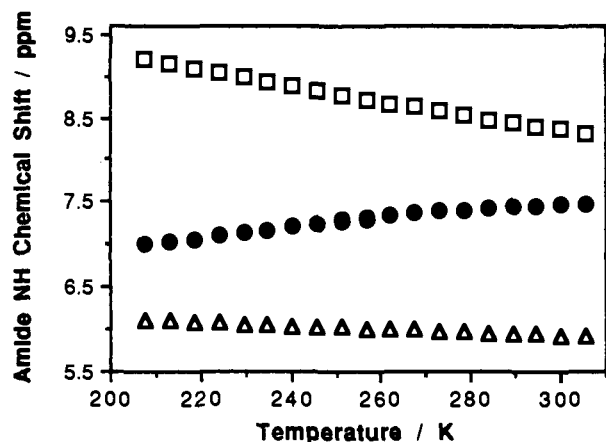

Figure 13. Amide proton NMR chemical shifts for 1 mM samples in CD_2Cl_2, as a function of temperature. H_a of triamide **1** (●); diamide ester **13** (□); amide ester **12** (△).
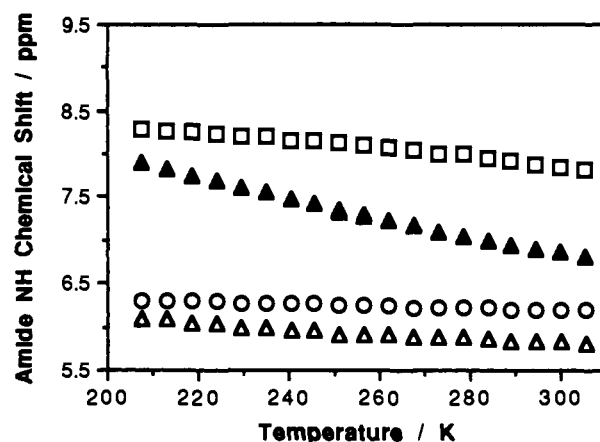
Figure 14. Amide proton NMR chemical shifts for 1 mM samples in CD_2Cl_2, as a function of temperature. H_b of triamide **1** (▲); diamide **3** (○); triamide **7** (□); C-terminal NH of **9** (△).

according to the IR data in Figure 4d, because there is little absorbance in the region 3390–3410 cm^{-1}.

Amide ester **12** and diamide ester **13** prove to be better choices for estimating $\Delta\delta NH_a/\Delta T$ of triamide **1** in the native and denatured states, respectively. It has been previously reported that the ester group of **12** does not engage in a C_5-type interaction with the amide proton;[21] however, the IR spectrum in Figure 12a shows maxima at 3452 and 3438 cm^{-1}, which may be assigned to a non-hydrogen-bonded N–H stretch and an N–H stretch stemming from a weak C_5-type interaction with the ester carbonyl. The breadth of the high-wavenumber band observed for **13** in Figure 12b also suggests the occurrence of some C_5-type interaction, although this molecule appears to be engaged largely in a six-membered-ring interaction. Despite these additional interactions in **12** and **13**, a potential source of error in the thermodynamic analysis, their behavior is closer to that expected for the limiting states of H_a of **1** than is the behavior of **10** and **11**. In each case, the ester group is expected to reproduce the inductive effects of the analogously positioned amide group of **1** on δH_a.

Figure 13 shows a juxtaposition of the $\Delta\delta NH/\Delta T$ signatures for **12**, **13**, and H_a of **1** (all samples 1 mM in CD_2Cl_2). At any given temperature, K_{eq} for the denatured vs native forms of **1** defined in Scheme II is given by eq 2:

$$K_{eq} = (\delta_{H_a} - \delta_{13})/(\delta_{12} - \delta_{H_a}) \tag{2}$$

where δ_{H_a} is the chemical shift of H_a of **1** at that temperature, δ_{13} is the chemical shift of the lone amide proton of **13** at that temperature (representing the limiting denatured state), and δ_{12} is the chemical shift of the lone amide proton of **12** at that temperature (representing the limiting native state).

Figure 14 shows a juxtaposition of the $\Delta\delta NH/\Delta T$ signatures for **3**, **7**, **9**, and H_b of **1** (all samples 1 mM in CD_2Cl_2). Using these data sets, K_{eq} as defined in Scheme II for the denatured vs the native forms of **1** at a given temperature can be calculated using eq 3:

$$K_{eq} = (\delta_{H_b} - \delta_n)/(\delta_7 - \delta_{H_b}) \tag{3}$$

where δ_{H_b} is the chemical shift of H_b of **1** at that temperature, δ_n is the chemical shift of the lone amide proton of **3** or **9** at that temperature (representing the limiting denatured state), and δ_7 is the chemical shift of the lone amide proton of **7** at that temperature (representing the limiting native state).

Figure 15 shows the results of van't Hoff analyses of the conformational equilibrium experienced by **1**, based upon eqs 2 and 3. These analyses were carried out using data obtained in the range 210–306 K with 1 mM samples of **1** and the reference
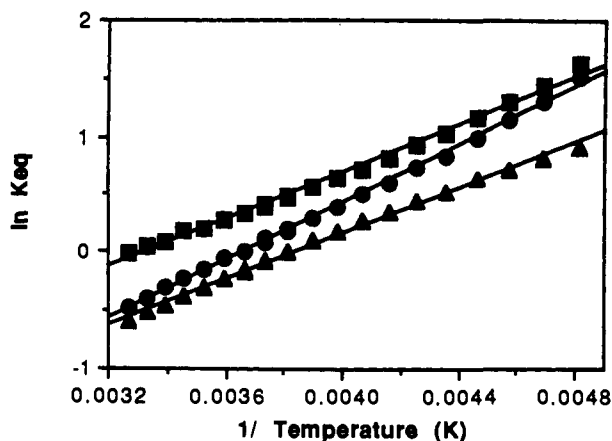
Figure 15. van't Hoff plots from amide proton NMR data obtained with 1 mM samples in CD_2Cl_2, 208–306 K (data shown in Figures 13 and 14). K_{eq} determined according to eq 2 in the text (▲); K_{eq} determined according to eq 3 (n = 3) in the text (●); K_{eq} determined according to eq 3 (n = 9) in the text (■). Each line represents the best fit to the van't Hoff equation (eq 1), respectively: $\Delta H°$ = –2.0 kcal/mol and $\Delta S°$ = –7.6 eu (correlation coefficient = 0.997); $\Delta H°$ = –2.5 kcal/mol and $\Delta S°$ = –9.0 eu (correlation coefficient = 0.998); $\Delta H°$ = –2.1 kcal/mol and $\Delta S°$ = –6.8 eu (correlation coefficient = 0.995).

Table II. Summary of Thermodynamic Parameters for Triamides **1** and **5**[a]

triamide	solvent	spectroscopic probe	$\Delta H°$ (kcal/mol)	$\Delta S°$ (eu)
1	CD_2Cl_2	$\Delta\delta NH_a/\Delta T$	–2.0	–7.6
1	CD_2Cl_2	$\Delta\delta NH_b/\Delta T$[b]	–2.5	–9.0
1	CD_2Cl_2	$\Delta\delta NH_b/\Delta T$[c]	–2.1	–6.8
1	$CDCl_3$	$\Delta\delta NH_a/\Delta T$	–1.7	–7.5
1	$CDCl_3$	$\Delta\delta NH_b/\Delta T$[b]	–2.0	–8.9
5	CD_2Cl_2	$\Delta\delta NH_b/\Delta T$[b]	–1.9	–6.4
5	CD_2Cl_2	N–H_b stretch	–1.5	–3.3

[a] Details of thermodynamic analyses are provided in the text. [b] Using diamide **3** as the reference for $\Delta\delta NH_b/\Delta T$ in the denatured state. [c] Using diamide **9** as reference for $\Delta\delta NH_b/\Delta T$ in the denatured state.
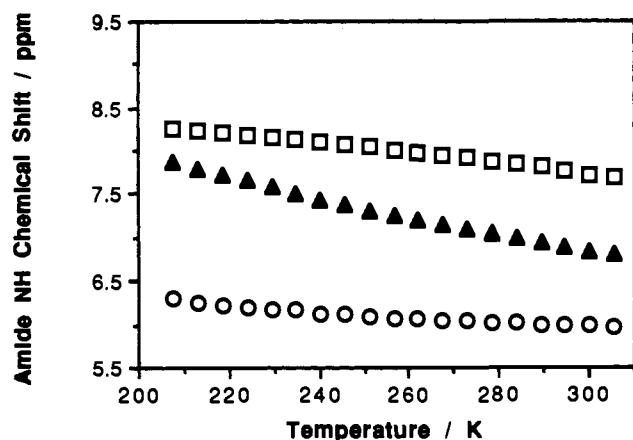

Figure 16. Amide proton NMR chemical shifts for 1 mM samples in CD_2Cl_2, as a function of temperature. H_b of triamide **5** (▲); major rotamer of triamide **8** (□); C-terminal amide proton of **14** (○).

compounds. In order to ensure that aggregation of **1** was not significant under these conditions, we carried out a parallel set of analyses using δNH_a and δNH_b values for **1** that had been linearly extrapolated to infinite dilution (Figures 2 and 3). (Data from 1 mM samples were used for all reference compounds in this second set of analyses; control experiments indicated that no significant aggregation of the references compounds occurred under these conditions.) For these parallel analyses, the differences in the derived $\Delta H°$ and $\Delta S°$ were consistently ≤0.1 kcal/mol and ≤0.2 eu, which supports our earlier conclusion that aggregation effects are negligible at 1.0 mM.
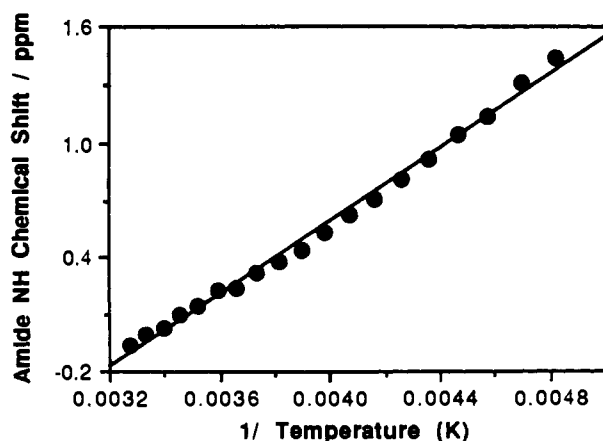

Figure 17. van't Hoff plot for denatured vs native **5** in CD_2Cl_2, based on amide proton NMR data shown in Figure 16, 208–306 K, with K_{eq} determined according to eq 1 in the text. The line represents the best fit to the van't Hoff equation (ln K_{eq} = $-\Delta H°/RT + \Delta S°/R$): $\Delta H°$ = –1.9 kcal/mol and $\Delta S°$ = –6.4 eu (correlation coefficient = 0.993).

Variations among the $\Delta H°$ and $\Delta S°$ values derived from the use of different model compounds (Figure 15; Table II) may be regarded as an indication of the level of error associated with the choice of reference compounds for δNH_a and δNH_b in the native and denatured states. Thus, for example, the difference between a secondary amide and a tertiary amide as seven-membered-ring hydrogen-bond acceptor (**9** vs **3** as model for H_b of **1** in the denatured state) does not appear to be significant. These analyses indicate the native state of **1** to be enthalpically favored in methylene chloride by 1.9–2.5 kcal/mol but entropically disfavored by 7.4–9.1 eu. The relatively good agreement between the values obtained from two independent data sets, that involving δNH_a and that involving δNH_b, strongly supports the validity of the assumptions underlying this thermodynamic analysis.

Thermodynamic Analysis of the Folding of Triamide 5. The folding of **5** in methylene chloride can be analyzed in terms of a two-state model analogous to that used for **1** (Scheme II). We carried out an NMR-based thermodynamic analysis based on H_b of **5**, using the lone amide proton resonance of the major rotamer of **8** to represent the limiting chemical shift for the native state and the C-terminal amide resonance of N-acetylalanine methylamide (**14**) to represent the limiting chemical shift for the denatured state. Figure 16 shows the $\Delta\delta NH/\Delta T$ signatures for H_b of **5**, the major rotamer of **8**, and the C-terminal amide proton of **14**. At any given temperature, the equilibrium constant for the two-state model is given by eq 4:

$$K_{eq} = (\delta_{H_b} - \delta_{14})/(\delta_8 - \delta_{H_b}) \qquad (4)$$

where δ_{H_b} is the chemical shift of H_b of **5** at that temperature, δ_{14} is the chemical shift of the C-terminal amide proton of **14** at that temperature, and δ_8 is the chemical shift of the amide proton of the major rotamer of **8** at that temperature. These K_{eq} values were used to construct the van't Hoff plot shown in Figure 17. This analysis implies that the native state is favored enthalpically by 2.0 kcal/mol but disfavored entropically by 6.4 eu relative to the denatured state in methylene chloride. As expected on the basis of the qualitative similarity of the $\Delta\delta NH/\Delta T$ data sets shown in Figure 6, the thermodynamic values for **5** in methylene chloride are similar to those derived for **1**.

A parallel thermodynamic analysis of the folding of **5** was carried out on the basis of the IR data shown in Figure 7. Only the band assigned to non-hydrogen-bonded N–H_b (the band at highest wavenumber in Figure 7) was used for this analysis; we assumed that H_b is completely free of intramolecular C=O···H—N hydrogen bonding in the denatured state and is completely hydrogen-bonded in the native state. (The lack of seven-membered-ring hydrogen bonding indicated by the room temperature IR spectrum of glycine derivative **9** (Figure 11a)
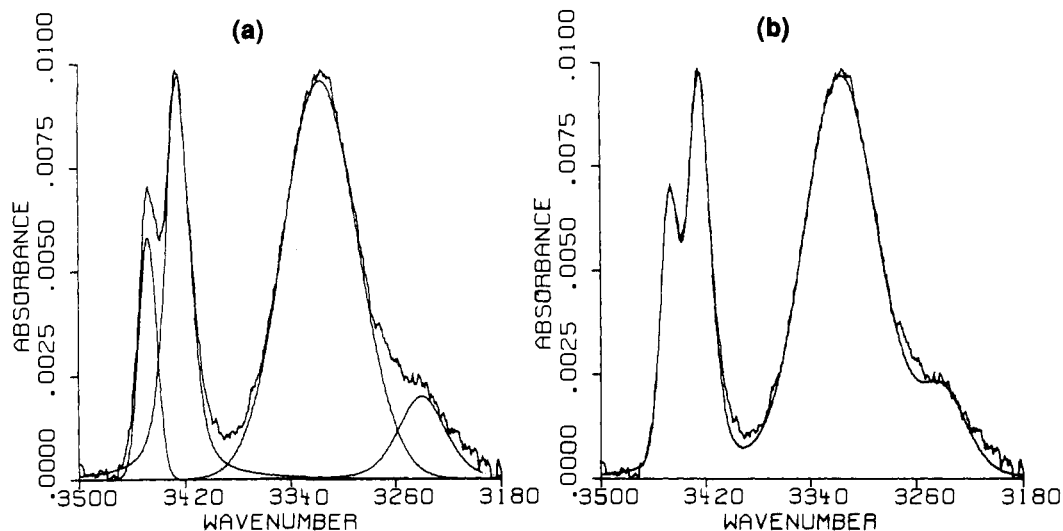
Figure 18. Representative spectral decomposition of the N–H stretch region of triamide **5** (1 mM in CH_2Cl_2, 255 K). (a) Four calculated bands superimposed on the observed spectrum: calculated maxima at 3448, 3425, 3316, and 3240 cm^{-1}. (b) Reconstructed spectrum superimposed on the observed spectrum. Details of the curve-fitting procedure are provided in the Experimental Section. The small band at 3240 cm^{-1} is tentatively assigned to a folding pattern in which H_a is simultaneously engaged in a six-membered ring hydrogen bond and a C_5 hydrogen bond with the alanine residue's carbonyl. This band diminishes as the temperature is lowered.

supports this assumption.) Because of partial band overlap, this analysis required the use of a curve fitting procedure for isolation of the non-hydrogen-bonded N–H_b stretch band (details of the curve fitting procedure are provided in the Experimental Section; a representative decomposition is shown in Figure 18).

The integrated extinction coefficient of the non-hydrogen-bonded N–H_b stretch band and the temperature dependence of that extinction coefficient were estimated by using IR data for lactic acid derivative **15**. (A 1 mM sample of **15** in CH_2Cl_2 shows only a single non-hydrogen-bonded N–H stretch band, 3451–3457 cm^{-1}, at all temperatures.) These extinction coefficient data were then used to calculate the absolute concentration of non-hydrogen-bonded N–H_b (denatured state) of **5** at each temperature. That portion of the total triamide concentration not accounted for in this way was attributed to the native state. The resulting temperature-dependent ratios of the denatured-to-native-state concentrations (K_{eq}) were used to construct the van't Hoff plot shown in Figure 19. On the basis of duplicate data sets for **5** and **15**, this analysis implies that the native state of **5** is enthalpically favored by 1.1–1.9 kcal/mol but entropically disfavored by 1.7–4.9 eu, relative to the denatured state, in CH_2-Cl_2. Addition of up to 30 mM D_2O did not affect the IR-derived $\Delta H°$ and $\Delta S°$ values. In light of the uncertainties associated with the spectral decomposition, we consider the average $\Delta H°$ to be in relatively good agreement with the value derived from the ^1H NMR-based analysis of **5** (Table II).

Folding Behavior of Triamide 1 in Chloroform. Figure 20 shows $\Delta\delta NH/\Delta T$ data for 1 mM samples of **1–3** and N-methylacetamide in $CDCl_3$. Triamide **1** appears to undergo a temperature-dependent change in folding pattern similar to that detected in CD_2Cl_2, particularly as judged by the fact that δNH_a increases at higher temperatures. Other IR and NMR data (not shown) are also consistent with the proposition that intramolecular hydrogen-bonding phenomena occurring in dilute chloroform solutions of **1–3** and related compounds are qualitatively similar to the behavior detected in methylene chloride.

The $\Delta\delta NH/\Delta T$ signatures for amides **3, 7, 12,** and **13** in $CDCl_3$ were used as references for thermodynamic analyses of the temperature-dependent changes in the folding of **1** (Scheme II), as previously described for CH_2Cl_2. Results are summarized in Figure 21 and Table II. The agreement between the two independent data sets in $CDCl_3$ is relatively good, and there is little variation between the thermodynamic values obtained in CD_2Cl_2 and $CDCl_3$.

Folding Behavior of Triamide 1 in Acetonitrile and DMSO.
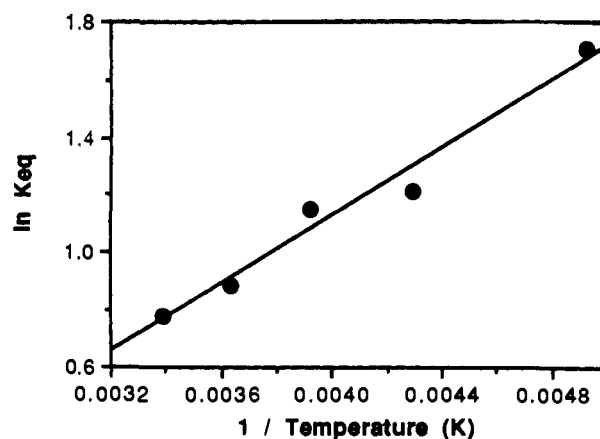

Figure 19. van't Hoff plot for denatured vs native **5** in CH_2Cl_2, based on the non-hydrogen-bonded N–H stretch band of H_b (Figure 7), 205–297 K. K_{eq} for the two-state equilibrium was calculated by assuming that H_b is completely hydrogen-bonded in the native state and that the portion of the total amide concentration not accounted for by the absorption of the non-hydrogen-bonded N–H_b band represents the concentration of the native state. The line represents the best fit to the van't Hoff equation ($\ln K_{eq} = -\Delta H°/RT + \Delta S°/R$): $\Delta H° = -1.2$ kcal/mol and $\Delta S° = -2.5$ eu (correlation coefficient = 0.971).

Figure 22 shows IR data for triamides **1** and **7**, diamide **3**, and diamide ester **13** in CH_3CN at room temperature. We have previously reported that a solvent-exposed N–H group in CH_3-CN gives rise to a stretch band in the vicinity of 3400 cm^{-1}.[7] Figure 22b shows that triamide **7** occurs largely in the nine-membered-ring hydrogen-bonded folding pattern in this solvent, but Figure 22c suggests that diamide **3** experiences little or no seven-membered-ring hydrogen bonding, and Figure 22d shows that diamide ester **13** experiences little six-membered-ring hydrogen bonding under these conditions. Triamide **1** has strong bands for both hydrogen-bonded and non-hydrogen-bonded N–H (Figure 22a), implying that at least one of the molecule's amide protons is experiencing considerable intramolecular N—H⋯O=C interaction. The behavior of **3, 7,** and **13** leads us to conclude that this intramolecular interaction in **1** involves predominantly the nine-membered-ring hydrogen bond. Thus, relative to methylene chloride (cf. Figures 4b, 10a, and 12b), acetonitrile appears to disrupt selectively the six-membered-ring hydrogen bond.

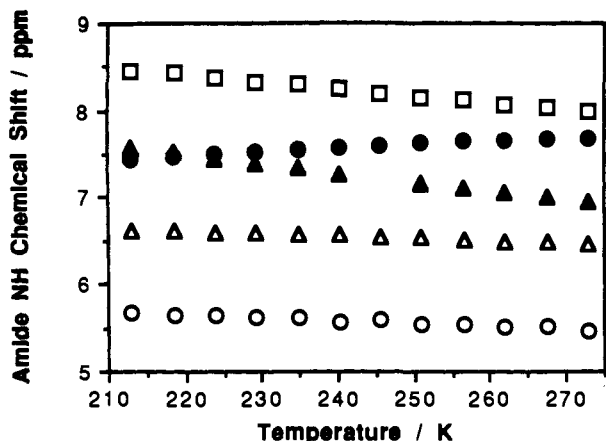Figure 23 shows the $\Delta\delta NH/\Delta T$ signatures in CD_3CN for H_a

Figure 20. Amide proton NMR chemical shifts of 1–3 and *N*-methylacetamide, 1 mM in $CDCl_3$, as a function of temperature. H_a of triamide 1 (●), H_b of triamide 1 (▲), diamide 2 (□), diamide 3 (△), *N*-methylacetamide (○).
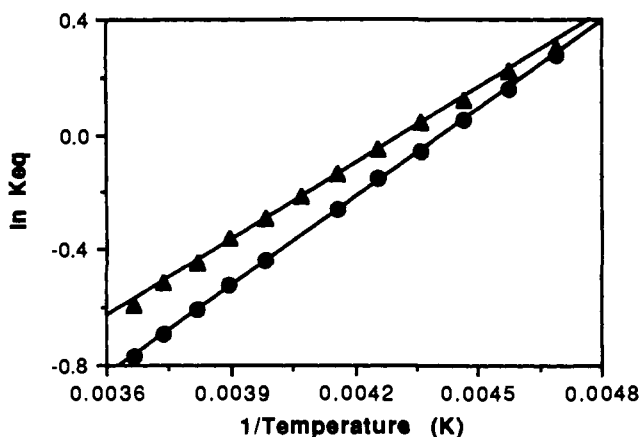

Figure 21. van't Hoff plots from amide proton NMR data obtained with 1 mM samples in $CDCl_3$, 213–273 K (data shown in Figure 20). K_{eq} determined according to eq 2 in the text (▲); K_{eq} determined according to eq 3 ($n = 3$) in the text (●). Each line represents the best fit to the van't Hoff equation (eq 1), respectively: $\Delta H° = -1.7$ kcal/mol and $\Delta S° = -7.5$ eu (correlation coefficient = 0.998); $\Delta H° = -2.0$ kcal/mol and $\Delta S° = -8.9$ eu (correlation coefficient = 1.000).

and H_b of triamide 1, diamide 3, triamide 7, diamide ester 13, and *N*-methylacetamide in CD_3CN (all samples 10 mM; intermolecular hydrogen bonding is negligible under these conditions[7]). The similarity between 3 and *N*-methylacetamide indicates that there is little or no seven-membered-ring hydrogen bonding at any temperature. Diamide ester 13 should be experiencing as much six-membered-ring hydrogen bonding as is possible under these conditions, and triamide 7 should be experiencing as much nine-membered-ring hydrogen bonding as is possible under these conditions. δNH_a of 1 is always farther upfield from δNH of 13 than δNH_b of 1 is from δNH of 7, supporting our hypothesis that acetonitrile destabilizes the six-membered-ring hydrogen bond, involving H_a, relative to the nine-membered-ring hydrogen bond, involving H_b.

Attempts to determine the thermodynamics of the folding process in acetonitrile through the use of $\Delta\delta NH/\Delta T$ data, analogous to the approach described above for methylene chloride and chloroform were unsuccessful: analyses based on H_a and H_b gave significantly different $\Delta H°$ and $\Delta S°$ values. This lack of agreement suggests that the behavior of 1 in acetonitrile cannot be described in terms of the simple two-state model summarized in Scheme II.

In DMSO, the N–H stretch region IR spectrum of 1 shows a single broad band, centered at 3280 cm^{-1} (10 mM, room temperature). A band at the same position is observed for 10 mM *N*-methylacetamide in DMSO. Because intramolecular

C=O···H—N interactions in 1 in CH_3CN or CH_2Cl_2 at room temperature give rise to bands >30 cm^{-1} higher (Figures 4d and 22a), we conclude that in DMSO the N–H groups of 1 are largely hydrogen-bonded to solvent rather than intramolecularly hydrogen bonded. We have previously reported similar observations for several derivatives of triamide 7.[5b] Apparently, the strongly hydrogen-bond-accepting nature of the sulfoxide oxygen prevents the occurrence of significant amounts of intramolecular hydrogen bonding in these triamides.

Discussion

We have used the intramolecular hydrogen-bonding interactions of amide protons H_a and H_b to tell us which folding patterns of 1 are populated in solution under various conditions. (The intramolecular hydrogen bonds also provide at least part of the driving force for folding, a separate point that will be discussed further below.) The use of hydrogen-bonding interactions for the characterization of folding behavior has several advantages, at least in relatively small molecules. Equilibrium among hydrogen-bonded and non-hydrogen-bonded states is slow on the IR time scale. Therefore, variable-temperature IR data can be used to determine the thermodynamic relationships ($\Delta H°$ and $\Delta S°$, from eq 1) between non-hydrogen-bonded and intramolecularly hydrogen-bonded states, provided that the molecule's behavior is adequately described by a two-state model and provided that IR band overlap is not a problem.[22] Secondary amide N–H stretch bands are particularly useful in the latter regard, because they occur in a relatively unobstructed region of the spectrum. In practice, overlap among N–H stretch bands usually limits IR-based analysis to systems containing one or two N–H moieties.[7,23]

^{1}H NMR-based analysis of intramolecular hydrogen-bonding interactions involving amides has the advantage, relative to IR-based analysis, that the resonances of large numbers of amide protons can usually be resolved from one another. ^{1}H NMR has two disadvantages relative to IR for detection of hydrogen bonding: (i) equilibration among hydrogen-bonded and non-hydrogen-bonded states is usually rapid on the NMR time scale; (ii) factors other than the extent of hydrogen-bond formation can influence the chemical shift of an amide proton in different conformational states. The latter effects can be accounted for, at least to some extent, through comparisons among homologous molecules containing limited structural variations. One can attempt to overcome interpretational ambiguities associated with the slow time scale of NMR measurements by correlation of NMR and IR data for molecules containing only one or two N–H groups.[7]

The "states" we distinguish by monitoring changes in N–H stretch bands and/or $\Delta\delta NH$ values may comprise multiple discrete conformations. We have been able to achieve reasonably good quantitative correlation of NMR- and IR-derived thermodynamic values for several di- and triamide systems,[7,24] including 5, which suggests that these two spectroscopic methods are similarly sensitive to the difference between "hydrogen-bonded" and "non-hydrogen-bonded" states. This correlation also suggests that these operationally defined states have a physical significance that transcends the methods used to detect them.

It is important to note that for an amide proton equilibrating between or among non-hydrogen-bonded and hydrogen-bonded states, the observed δNH is a *linearly* weighted average of the δNHs of the contributing states. NOESY (or ROESY) measurements represent an alternative NMR-based strategy for the detection of compact conformations of flexible molecules in

---

(22) A number of two-state analyses of intramolecular hydrogen bonding, based on O–H stretch IR data, have been reported; see: Aaron, H. S. *Top. Stereochem.* **1980**, *11*, 1 and references therein.

(23) Boussard, G.; Marraud, M. *J. Am. Chem. Soc.* **1985**, *107*, 1825 and references therein.

(24) Liang, G.-B.; Desper, J. M.; Gellman, S. H. *J. Am. Chem. Soc.* **1993**, *115*, 925.
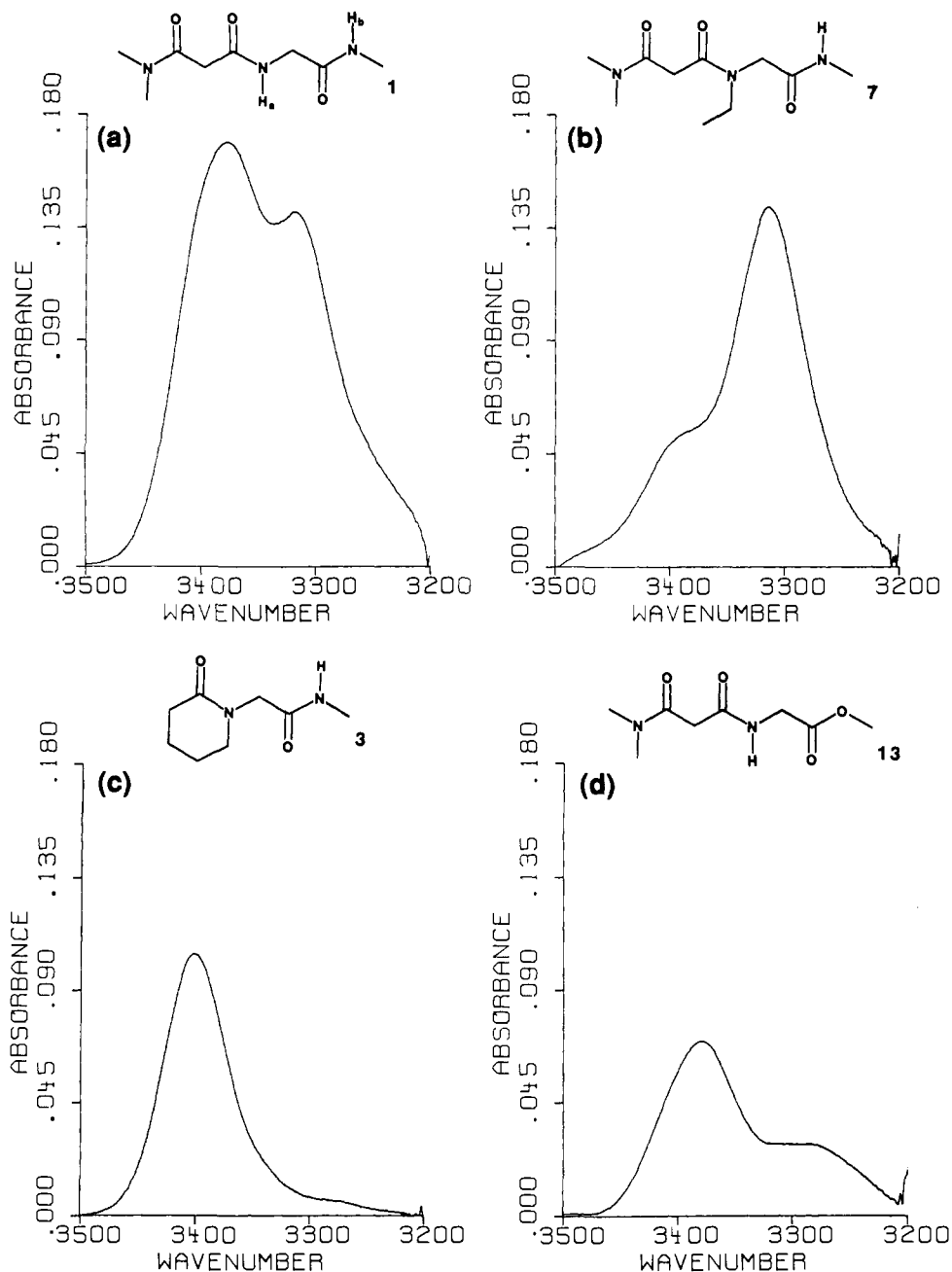
Figure 22. N–H stretch region FT-IR spectral data for 10 mM amide samples in CH_3CN at 297 K, after subtraction of the spectrum of pure CH_3CN at the same temperature. (a) Triamide **1** (absorption maxima at 3380 and 3318 cm^{-1}); (b) triamide **7** (absorption maxima at 3395 and 3313 cm^{-1}); (c) diamide **3** (absorption maximum at 3400 cm^{-1}); (d) diamide ester **13** (absorption maxima at 3379 and 3285 cm^{-1}).

solution, but in this case, signals stemming from dipolar coupling are *nonlinearly* weighted averages of the coupling in contributing states (because dipolar coupling exhibits an inverse sixth-power dependence on distance). Therefore, thermodynamic analysis based on variable temperature NOESY (or ROESY) experiments would be more susceptible to artifacts arising from minor populations than is analysis based on δNH.

Qualitative Behavior of Triamide 1 in Methylene Chloride. Our data strongly support the folding hypothesis summarized in Scheme II. One key feature of this hypothesis is that at low temperatures **1** favors a conformation in which only a single C=O···H—N hydrogen bond occurs, in a nine-membered ring. Variable-temperature IR data for **5** and **6** (Figures 7 and 9) are particularly important in this regard, since they show that for both triamides the amount of non-hydrogen-bonded H_b decreases at lower temperatures, and that the amount of non-hydrogen bonded H_a increases at lower temperatures. This feature of our hypothesis also explains the unusual observation that $\Delta\delta NH_a/\Delta T > 0$ for **1** and **5**, and, to a lesser extent, for **6** (Figures 1, 6

and 8). These data are not consistent with the hypothesis that both H_a and H_b are intramolecularly hydrogen bonded in the most stable conformation of **1** in methylene chloride (e.g., as in **1b** or **1e**).[9,10]

Comparison of the NMR data for H_b of **1** with data for the amide proton of **3** and for the C-terminal amide proton of **9** (Figure 14) indicates that a seven-membered-ring N—H···O=C interaction cannot explain the large amount of hydrogen bonding experienced by H_b at low temperatures. We therefore conclude that the intramolecular hydrogen bond must occur in a nine-membered ring. The plausibility of this proposal is enhanced by the observation of this nine-membered-ring interaction in a crystal structure of **1**.[5] The data we have presented here do not rule out the possibility that H_b is engaged in a bifurcated hydrogen bond at low temperatures in methylene chloride, involving simultaneous seven- and nine-membered-ring interactions (i.e., **1f** rather than **1c**, Chart II); however, comparison of amide I-region IR data from ^{13}C-labeled derivatives of **7** and related compounds indicates that
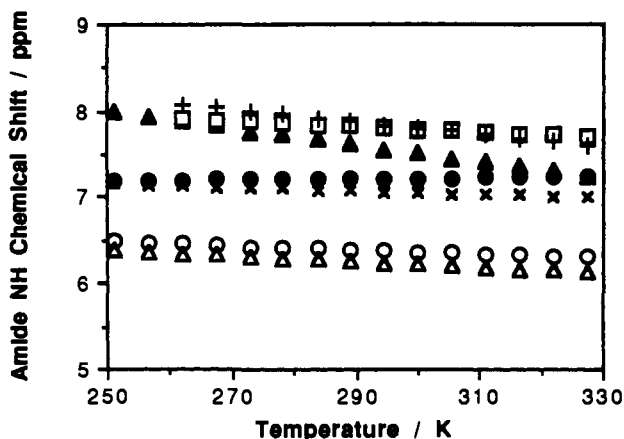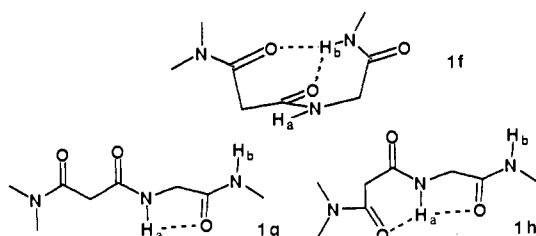
Temperature-Dependent Folding Pattern of a Synthetic Triamide

J. Am. Chem. Soc., Vol. 115, No. 10, 1993 4241

Figure 23. Amide proton NMR chemical shifts of **1, 2, 3, 7, 13**, and *N*-methylacetamide, 10 mM in CD_3CN, as a function of temperature. H_a of triamide **1** (●), H_b of triamide **1** (▲), diamide **2** (×), diamide **3** (○), triamide **7** (+), diamide ester **13** (□), *N*-methylacetamide (△).

Chart II

that only the nine-membered-ring interaction occurs in triamide **7** in this solvent.[8]

Variable-temperature IR and ¹H NMR data for **1, 5**, and **6** suggest that state **1a** (or its equivalent for **5** or **6**) is increasingly populated at higher temperatures, at least through the liquid range of methylene chloride. The observation that $\Delta\delta NH_a/\Delta T$ > 0 is particularly revealing, since the most likely explanation for such behavior is that H_a experiences an increasing amount of intramolecular hydrogen bonding at higher temperatures. In principle, H_a can experience both five- and six-membered-ring N—H···O=C interactions (cf. **1g** and **1h**), but data from model compounds suggest that the five-membered-ring interaction does not occur to a significant extent in **1**. The lone N–H stretch band observed in the IR spectrum of diamide **10** at 3406 cm⁻¹ (Figure 11b) is characteristic of the five-membered-ring interaction.[21] Since there is little absorbance in the region 3390–3410 cm⁻¹ in the spectrum of **1** (high or low temperature, Figure 4d), we rule out the existence of a significant population of **1g**. In contrast, triamide **11** shows a large band at 3394 cm⁻¹ (Figure 11b), which may be assigned to structure **11a** (Chart III). A second, broader band is observed at 3290 cm⁻¹ for **11**, which may arise from either **11b** or **11c**. The fact that this band is at somewhat lower energy than the hydrogen-bonded N–H band maximum in the spectrum of **2** (3303 cm⁻¹; Figure 4a), which represents an isolated six-membered ring, may suggest that **11c** is the correct structure. The hydrogen-bonded maximum of **1** under these conditions, however, is 3319 cm⁻¹ (Figure 4d), indicating that **1h** is not a major species in solution. Curve fitting analysis of the IR data for triamide **5** indicates the presence of a minor band at ca. 3240 cm⁻¹ (Figure 18). This minor band, which diminishes at lower temperatures, may arise from a minor population of the folding pattern of **5** analogous to **1h**.

Thermodynamic Parameters. One of our goals has been to determine whether thermodynamic parameters for the folding of **1** can be reliably extracted from variable-temperature spectroscopic data. Efforts to obtain thermodynamic information on

Chart III
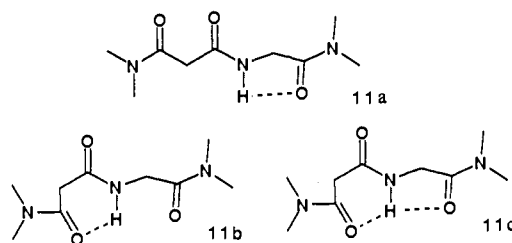
folding processes in small molecules have been relatively rare,[22,25] and in virtually every case the analysis has been based on a single data set. This type of study is subject to a variety of errors. (In our NMR-based approach, for example, errors could arise from limitations in the fidelity with which the model compounds represent $\Delta\delta NH_a/\Delta T$ and $\Delta\delta NH_b/\Delta T$ in the denatured and native states of **1** or **5**.) We therefore believed it necessary to determine van't Hoff $\Delta H°$ and $\Delta S°$ values from two independent data sets, so that the level of agreement between the parallel analyses would reveal the accuracy and precision of these values. For diamide **16**, which can experience only one intramolecular hydrogen bond, we have previously demonstrated a quantitative correlation between van't Hoff thermodynamic parameters obtained from independent IR- and ¹H NMR-based analyses,[7] and we have recently observed similar correlations with other synthetic diamides.[24]

As summarized in Table II, we have determined thermodynamic parameters for three related processes, temperature-dependent changes in the folding pattern of (i) **1** in methylene chloride (two independent sets of NMR data); (ii) **1** in chloroform (two independent sets of NMR data); and (iii) **5** in methylene chloride (one set of NMR data and one set of IR data). The variations in $\Delta H°$ and $\Delta S°$ values observed for each parallel analysis are greater than uncertainties arising from the reproducibility of the IR and NMR measurements. In each case, the values determined by independent approaches agree reasonably well with one another, particularly for $\Delta H°$. The relatively poorer agreement for $\Delta S°$ may be result from the fact that this value is derived from the intercept of a van't Hoff plot, while $\Delta H°$ is derived from the slope. Intercepts are inherently more subject to error (e.g., in determination of total concentration) than are slopes. The NMR- and IR-based values for **5** show the poorest agreement with one another, which may reflect the intrinsic imprecision of the curve-fitting procedure employed for the IR analysis and/or imperfection in the model-derived extinction coefficient. In addition, the IR-based analysis involves the assumption that there is no intramolecular hydrogen bonding at H_b of **5** in the denatured state, while the NMR-based analysis allows for minor amounts of folding patterns containing hydrogen bonds to H_b in this state.

Our ability to determine thermodynamic parameters for equilibria between alternative hydrogen-bonded states from $\Delta\delta NH/\Delta T$ data is noteworthy because there are two different possible origins of the temperature dependence observed for an amide proton chemical shift. In nonpolar solvents, the non-hydrogen-bonded and intramolecularly hydrogen-bonded states of an amide proton will often have significantly different chemical shifts ($\Delta\delta$ values of 2–3 ppm are not uncommon).[7,26] If an amide proton is equilibrating between a non-hydrogen-bonded state and a hydrogen-bonded state in the temperature range under exam-

(25) Two groups have attempted to determine the thermodynamic parameters for seven-membered-ring N—H···O=C hydrogen-bond formation in small peptides by variable-temperature IR measurements: (a) Mizushima, S.; Shimanouchi, T.; Tsuboi, M.; Arakawa, T. *J. Am. Chem. Soc.* **1957**, *79*, 5357. (b) Portnova, S. L.; Bystrov, V. F.; Tsetlin, V. I.; Ivanov, V. T.; Ovchinnikov, Y. A. *Zh. Obshch. Khim.* **1968**, *38*, 428 (424 in the English translation). Subsequent reports have shown these two analyses to have been in error, see ref 11e.

(26) Monoamide aggregation in $CDCl_3$ and CCl_4 has been previously quantified by monitoring the amide proton chemical shift, see: (a) LaPlanche, L. A.; Thompson, H. B.; Rogers, M. T. *J. Phys. Chem.* **1965**, *69*, 1482. (b) Graham, L. L.; Chang, C. Y. *J. Phys. Chem.* **1971**, *75*, 776.

ination and if the position of the equilibrium is altered by changes in temperature (i.e., $\Delta H^\circ \neq 0$ (see eq 1)), then at least part of the change in δNH as a function of temperature will arise from the change in the equilibrium mixture of non-hydrogen-bonded and hydrogen-bonded forms. It is this component of $\Delta\delta$NH/ΔT that provides access to the thermodynamic parameters we seek. The amide proton resonance can, however, also manifest characteristic temperature dependences in each of its limiting states (non-hydrogen-bonded and intramolecularly hydrogen-bonded), and our thermodynamic analysis must correct for these sources of temperature dependence. Non-hydrogen-bonded amide protons generally show small temperature dependences in chlorocarbon solvents (ca. -2×10^{-3} ppm/K).[7,12c] It has usually been assumed by peptide chemists that completely intramolecularly hydrogen-bonded amide protons also show $\Delta\delta$NH/ΔT values (e.g., $\leq -2 \times 10^{-3}$ ppm/K),[27] but this assumption is not always correct. We have shown that for a flexible diamide, $\Delta\delta$NH/ΔT for the completely hydrogen-bonded state is ca. -5×10^{-3} ppm/K.[7] Adrian and Wilcox have recently reported a value of -6.6×10^{-3} ppm/°C for an intermolecular N—H$\cdots$O=C hydrogen bond (2-aminopyrimidine to a carboxylic acid) in $CDCl_3$.[17] (The temperature dependence of δNH for a fully hydrogen-bonded proton has been attributed to an increasing population of vibrationally excited states of the hydrogen bond; because the hydrogen bond potential is shallow and anharmonic, the readily accessible excited states have longer average hydrogen bond lengths.[28]) Our approach succeeds in isolating that portion of the observed $\Delta\delta$NH/ΔT that arises from changes in the equilibrium between non-hydrogen-bonded and hydrogen-bonded states because the intrinsic temperature dependences of δNH in those limiting states are accounted for by the $\Delta\delta$NH/ΔT signatures of the model compounds we employ.

Solvent Effects. The folding behavior of **1** in chloroform is quite similar to that in methylene chloride (Table II). Since intramolecular dipolar attractions probably constitute the principal drive for folding, the similarity is not surprising. Chloroform is somewhat less polar than methylene chloride (dielectric constants at room temperature are 4.8 and 9.1, respectively), which might enhance hydrogen-bonding attraction in the former;[29] however, chloroform is a more effective hydrogen-bond donor than methylene chloride (both are weak hydrogen-bonding partners compared to amides).[30] Our data suggest that chloroform's ability to provide stiffer competition for the hydrogen-bonding attentions of the oxygen atoms of **1** may offset the greater polarity of methylene chloride.

Acetonitrile is significantly more polar than either of the chlorocarbons, and the nitrile group is a moderate hydrogen-bond acceptor. (Studies of intermolecular hydrogen bonding have shown that amides are stronger acceptors than nitriles.[31]) We have previously reported that intramolecular hydrogen bonding detected among several flexible diamides dissolved in methylene chloride is no longer detectable when acetonitrile is used as solvent.[7] IR data show that this solvent also severely disrupts intramolecular hydrogen bonding in the six- and seven-membered rings of **13** and **3** (compare Figure 22d to 12b and Figure 22c to 4b). The nine-membered-ring N—H$\cdots$O=C hydrogen bond of triamide **7**, however, remains largely intact in this more interactive solvent. For triamide **1**, the strongest band in CH_3CN arises from a solvent-exposed N–H, but there is clearly a significant amount of intramolecular N—H$\cdots$O=C interaction (compare band proportions in Figures 22a and 22d). Comparison to the behavior of **13** and **3** suggests that this intramolecular hydrogen bonding stems largely from a nine-membered-ring interaction.

Acetonitrile's ability to disrupt the six-membered-ring N—H$\cdots$O=C hydrogen bond more effectively than the nine-membered-ring interaction is consistent with our earlier proposal that the hydrogen bond in the analogous six-membered ring of diamide **2** has a relatively small enthalpy of formation because of poor geometry (nonlinear N—H$\cdots$O angle).[7]

^{1}H NMR data suggest that **1** undergoes temperature-dependent changes in its folding pattern in acetonitrile that are qualitatively similar to those occurring in chlorocarbon solvents (Figure 23). Attempts to determine thermodynamic parameters for the folding process in CD_3CN using $\Delta\delta$NH/ΔT data for **1** and model compounds gave significantly different ΔH° and ΔS° values for analyses based on H_a and H_b. This inconsistency suggests that the behavior of **1** in acetonitrile does not conform to a two-state model.

In a DMSO solution of **1**, no intramolecular N—H$\cdots$O=C interactions could be detected spectroscopically. Since these types of hydrogen bonds are expected to be no more favorable than N—H$\cdots$O=S hydrogen bonds to solvent,[31] it is not surprising that competition from DMSO disrupts the intramolecular interactions in the flexible triamide.

Implications Regarding the Conformation-Directing Role of Hydrogen Bonds. We have shown that the most enthalpically favorable folding pattern of a flexible triamide in relatively nonpolar solvents is not determined by maximizing hydrogen-bonded pairing of N—H and C=O groups. There are probably several factors that favor **1c** over **1b**, including (i) the superior hydrogen-bond geometry allowed by the nine-membered ring relative to the six- and seven-membered rings;[32] (ii) the inherent torsional preferences of the covalent bonds that connect the hydrogen-bond donor and acceptor;[7] and (iii) other sources of intramolecular dipolar interaction in **1c**. (With regard to this last point, we have recently noted that a survey of malonamide fragments found in crystal structures indicates a tendency for the carbonyls to orient perpendicular to one another.[5c] This tendency could result from a dipolar repulsion and should promote adoption of folding pattern **1c**. Our own crystallographic data for **1** and several derivatives of **7** suggest that there may be a weak dipolar attraction between H_b and the central amide nitrogen in folding pattern **1c**.[5c]) Whatever combination of forces is responsible for the observed folding preference, the result is important because it demonstrates that the conformational stability of polar molecules in environments of low polarity cannot be predicted simply by anticipating the largest number of hydrogen bonds.

The interior of a folded protein is postulated to be a microenvironment of considerably lower dielectric than bulk aqueous solution.[33] It has been suggested that the drive to maximize the number of hydrogen bonds inside folded proteins constitutes a significant structure-specifying force.[34] Although the covalent connectivity between amide groups in **1** is not completely natural (there are no malonic acid residues in proteins), our results show in a general way that competing nonbonded forces can lead a molecule to prefer conformations containing fewer hydrogen bonds. We have recently reported analogous behavior in more biologically relevant molecules: the most enthalpically favorable folding patterns of Pro-Gly, Pro-Ala, and Pro-Val dipeptides in methylene chloride contain a single ten-membered-ring N—H$\cdots$O=C hydrogen bond rather than two seven-membered-ring hydrogen bonds.[6b] Although the enthalpic differences between folding patterns observed for **1**, **5**, and the Pro-X dipeptides are small (≤ 2.5 kcal/mol), these numbers are

(27) Kessler, H. *Angew. Chem., Int. Ed. Engl.* **1982**, *21*, 512.

(28) Muller, N.; Reiter, R. C. *J. Chem. Phys.* **1965**, *42*, 3265.

(29) (a) Klotz, I. M.; Franzen, J. S. *J. Am. Chem. Soc.* **1962**, *84*, 3461. (b) Franzen, J. S.; Stephen, R. E. *Biochemistry* **1963**, *2*, 1321.

(30) Sheridan, J. P.; Martire, D. E.; Tewari, Y. B. *J. Am. Chem. Soc.* **1972**, *94*, 3294.

(31) Arnett, E. M.; Mitchell, E. J.; Murty, T. S. S. R. *J. Am. Chem. Soc.* **1974**, *96*, 3875.

(32) Surveys of crystallographic data indicate that linearity is preferred for the N—H$\cdots$O angle of an amide-to-amide hydrogen bond: (a) Baker, E. N.; Hubbard, R. E. *Prog. Biophys. Molec. Biol.* **1984**, *44*, 97 and references therein. (b) Taylor, R.; Kennard, O.; Versichel, W. *Acta Crystallogr.* **1984**, *B40*, 280.

(33) For leading references, see: (a) Gilson, M. K.; Honig, B. H. *Nature* **1987**, *330*, 84. (b) Rodgers, K. K.; Sligar, S. G. *J. Am. Chem. Soc.* **1991**, *113*, 9419.

(34) Shirley, B. A.; Stanssens, P.; Hahn, U.; Pace, C. N. *Biochemistry* **1992**, *31*, 725 and references therein.

significant in light of the fact that the folded states of many globular proteins are stabilized by no more than 10 kcal/mol relative to their denatured states under physiological conditions.[35]

While hydrogen bonding almost certainly plays a major role in holding biomolecular complexes together and specifying biopolymer folding patterns, we suggest that chemists and biochemists may tend to overemphasize the role of hydrogen bonds in these and related phenomena. A biased affection for hydrogen bonds could arise from their detectability: hydrogen-bond formation is often signaled by clear spectroscopic changes in solution,[36] and there are accepted parameters for identifying hydrogen-bond formation in the solid state.[37] In contrast, the non-bonded forces that can oppose hydrogen-bond formation, e.g., countervailing torsional strain, are not readily visualized in solution or in the solid state. The misleading predictions for **1** and **3** in methylene chloride provided by AM1[10] and AMBER/MacroModel calculations[9] suggest that the tendency to overestimate the energetic significance of hydrogen-bond formation has been incorporated into these empirically derived computational methods. Structural and thermodynamic characterization of the behavior of small molecules in solution should continue to provide information that tests computational methods and the chemist's intuition.

Experimental Section

All melting points are uncorrected. THF was freshly distilled from sodium benzophenone ketyl under N_2. Triethylamine was distilled before use, and DMF was stored over 4-Å sieves. Reagents were used as obtained from commercial suppliers. For Boc removal, 4 N HCl in dioxane from Pierce Chemical Co. was used. The syntheses of compounds **1**,[6b] **2**,[7] **9**,[21] **10**,[21] **12**,[21] **13**,[6b] **14**,[21] and **15**[21] have been reported previously. Routine ^{1}H NMR spectra were obtained on a Bruker WP-200 spectrometer and are referenced to residual protonated NMR solvent. Routine ^{13}C NMR spectra were obtained on either a Bruker WP-270 or a Bruker AM-500 spectrometer and are referenced to the NMR solvent. For ^{1}H NMR and ^{13}C NMR spectra in which two rotamers are reported, not all signals for the minor rotamer are accounted for, presumably as a result of overlap with signals attributed to the major rotamer. High-resolution electron impact ionization mass spectroscopy was performed on a Kratos MS-80. Elemental analyses were performed at Galbraith Laboratories. Routine FT-IR spectra were recorded at room temperature on either a Nicolet 740 or a Mattson Polaris spectrometer. Column chromatography was carried out by using low N_2 pressure with 230–400 mesh silica gel 60 from EM Science. Columns eluted with low percentages of MeOH in CHCl$_3$ were slurry-packed after the slurry had been stirred with the eluant for at least 1 h. Fresh solvent was then passed through the column continuously until subtle changes in the gray hue of the silica had moved completely through the column bed. Preequilibration was essential for optimal resolution. Amides used for spectroscopic experiments were estimated to be >95% pure on the basis of 500-MHz ^{1}H NMR spectra.

Diamide 3. To a mixture of 0.50 g (12.5 mmol) of a 60 wt % sodium hydride dispersion in oil and 5 mL of DMF was added slowly a solution of 1.0 g (10 mmol) of valerolactam in 5 mL of DMF, resulting in a thick slurry. After being stirred under N_2 for 1 h, the mixture was cooled to 0 °C and 1.1 mL (12 mmol) methyl bromoacetate was slowly added. The resulting brown solution was stirred at room temperature for 2.5 h, and then 1 mL of acetic acid was added, and the solution was allowed to stand for 2.5 h. After evaporation of solvent, the brown slurry was partitioned between 10 mL of H$_2$O and 15 mL of EtOAc, and the aqueous layer was extracted with several portions of EtOAc. The combined organic layers were concentrated to an orange syrup, which was partially purified by SiO$_2$ column chromatography eluting with EtOAc and then 2% MeOH in CHCl$_3$ to afford the slightly impure lactam ester in 39% crude yield: ^{1}H NMR (CDCl$_3$) δ 4.10 (s, 2 H, N*CH$_2$*C═O), 3.72 (s, 3 H, OC*H$_3$*), 3.4–3.3 (m, 2 H, NC*H$_2$*), 2.45–2.35 (m, 2 H, C*H$_2$*C═O), 1.9–1.8 (m, 4 H, (C*H$_2$*)$_2$). The material was carried on without further purification.

To a solution of 0.43 g (2.5 mmol) of the crude lactam ester in 25 mL of methylamine–saturated MeOH was added 15 mg (0.3 mmol) of sodium

cyanide. After the solution was stirred for 70 h at room temperature, solvent was evaporated and the residue was taken up in CHCl$_3$. Solids were removed by filtration, and the filtrate was evaporated to a syrup, which, upon purification by SiO$_2$ column chromatography eluting with 3% MeOH in CHCl$_3$, afforded the desired diamide as an off-white solid (0.39 g, 36% overall yield): mp 75–76.5 °C; ^{1}H NMR (CDCl$_3$) δ 6.54 (br, 1 H, NH), 3.95 (s, 2 H, NC*H$_2$*C═O), 3.43–3.37 (m, 2 H, NC*H$_2$*), 2.75 (d, J = 4.9 Hz, 3 H, NHC*H$_3$*), 2.42–2.39 (m, 2 H, C*H$_2$*C═O), 1.89–1.75 (m, 4 H, (C*H$_2$*)$_2$); ^{13}C NMR (CDCl$_3$) δ 170.8, 169.3, 51.7, 49.6, 32.1, 25.9, 23.0, 21.1; IR (0.001 M in CH$_2$Cl$_2$) 3447 (NH), 3352 (NH), 1678 (amide I), 1634 (amide I), 1556 (amide II), 1536 (amide II) cm^{-1}; EI MS m/e 170.1055, calcd for C$_8$H$_{14}$N$_2$O$_2$ 170.1055. Anal. Calcd for C$_8$H$_{14}$NO: C, 56.45; H, 8.29; N, 16.46. Found: C, 56.82; H, 8.17; N, 16.51.

N-Methylcyclohexylacetamide (4). To a solution of 0.28 g (2 mmol) of cyclohexylacetic acid in 15 mL of THF was added 0.35 g (3 mmol) of N-hydroxysuccinimide and 0.512 g (2.5 mmol) of dicyclohexylcarbodiimide; a white precipitate formed within 15 min. After the mixture had been stirred under N_2 for 1 h, 0.41 g (6 mmol) of methylamine hydrochloride and 1 mL of triethylamine were added, and the slurry was stirred under N_2 for 20 h. The precipitate was then removed by gravity filtration. After concentration of the filtrate, the crude product was purified by SiO$_2$ column chromatography eluting with 50–100% EtOAc in hexane to afford 0.13 g (42% yield) of the desired amide as a white solid: mp 94.5–95 °C; ^{1}H NMR (CDCl$_3$) δ 5.45 (br, 1 H, NH), 2.80 (d, J = 4.9 Hz, 3 H, NHC*H$_3$*), 2.02 (d, J = 6.9 Hz, 2 H, C*H$_2$*C═O), 1.9–1.7 (m, 5 H, aliphatic CH), 1.4–0.8 (m, 6 H, aliphatic CH); IR (0.001 M in CH$_2$Cl$_2$) 3460 (NH), 1669 (amide I), 1520 (amide II) cm^{-1}; EI MS m/e 155.1301, calcd for C$_9$H$_{17}$NO 155.1310. Anal. Calcd for C$_9$H$_{17}$NO: C, 69.63; H, 11.04; N, 9.02. Found: C, 69.98; H, 10.78; N, 8.95.

Triamide 5. To a solution of 0.26 g (2 mmol) of the mono-*N*,*N*-dimethylamide of malonic acid[7] in 10 mL of THF was added 0.35 g (3 mmol) of N-hydroxysuccinimide and 0.52 g (2.5 mmol) of dicyclohexylcarbodiimide; a white precipitate quickly formed. After the solution was stirred under N_2 for 2 h, a mixture of 0.7 mL of triethylamine (5 mmol) and alanine methylamide hydrochloride (obtained from the reaction of 0.38 g (2 mmol) of N-(*tert*-butoxycarbonyl)alanine methylamide with 5 mL of 4 N HCl in dioxane; dioxane was removed before subsequent reaction) in 15 mL of DMF was added. The resulting slurry was stirred under N_2 for 21 h, and the precipitate was then removed by gravity filtration. After concentration of the filtrate, the crude product was purified by SiO$_2$ column chromatography eluting with 4% MeOH in CHCl$_3$ to afford slightly impure material in 60% yield. Recrystallization from dichloroethane afforded 0.18 g (41% yield) of triamide **5** as a white crystalline solid: mp 160.5–162.5 °C; ^{1}H NMR (CDCl$_3$) δ 7.70 (br, 1 H, N*H*CH), 6.77 (br, 1 H, N*H*CH$_3$), 4.48 (p, J = 7.3 Hz, 1 H, CH), AB δ$_A$ 3.37, δ$_B$ 3.32 (J_{AB} = 16 Hz, 2 H, C*H$_2$*(C═O)$_2$), 3.05 (s, 3 H, NC*H$_3$*), 2.99 (s, 3 H, NC*H$_3$*), 2.80 (d, J = 4.8 Hz, 3 H, NHC*H$_3$*), 1.41 (d, J = 7.2 Hz, 3 H, CHC*H$_3$*); ^{13}C NMR (CDCl$_3$) δ 172.4, 168.1, 166.6, 49.1, 40.0, 37.6, 35.7, 26.3, 17.5; IR (0.001 M in CH$_2$Cl$_2$) 3449 (NH), 3426 (NH), 3323 (NH), 1680 (amide I), 1670 (amide I), 1637 (amide I), 1555 (amide II), 1538 (amide II), 1518 (amide II) cm^{-1}; EI MS m/e 216.1354, calcd for C$_9$H$_{17}$N$_3$O$_3$ 216.1348. Anal. Calcd for C$_9$H$_{17}$N$_3$O$_3$: C, 50.22; H, 7.96; N, 19.52. Found: C, 50.22; H, 7.69; N, 18.79.

Triamide 6. To a solution of 0.7 g (4 mmol) of N-(*tert*-butoxycarbonyl)glycine in 30 mL of THF was added 0.69 g (6 mmol) of N-hydroxysuccinimide and 1.03 g (5 mmol) of dicyclohexylcarbodiimide; a white precipitate quickly formed. After stirring under N_2 for 1 h, 0.6 g (4 mmol) of 1-adamantanamine was added, and the mixture was stirred for 24 h. Solids were removed by gravity filtration, and the filtrate was concentrated to a thick syrup. Purification by SiO$_2$ column chromatography eluting with 2% MeOH in CHCl$_3$ afforded N-(*tert*-butoxycarbonyl)glycine 1-adamantylamide as an extremely viscous, colorless oil that entrapped large amounts of solvent (1.2 g, 98% crude yield): ^{1}H NMR (CDCl$_3$) δ 5.7 (br, 1 H, NH), 5.2 (br, 1 H, NH), 3.65 (d, J = 5.7 Hz, 2 H, NHC*H$_2$*C═O), 2.07 (br, 3 H, (CH)$_3$), 1.98 (br, 6 H, (CH$_2$)$_3$), 1.67 (br, 6 H, (CH$_2$)$_3$), 1.44 (s, 9 H, (CH$_3$)$_3$). This material was used without further purification.

Triamide **6** was prepared from the mono-*N*,*N*-dimethylamide of malonic acid and N-(*tert*-butoxycarbonyl)glycine 1-adamantylamide by a procedure analogous to the preparation of triamide **5**. The crude product was purified by several passes over a SiO$_2$ chromatography column eluting with EtOAc and then 3–4% MeOH in CHCl$_3$ to afford the desired triamide **6** as a white solid in 33% yield: mp 141.5–143 °C; ^{1}H NMR (CDCl$_3$) δ 7.97 (br, 1 H, N*H*CH$_2$), 6.15 (s, 1 H, NHC), 3.83 (d, J = 5.7 Hz, 2 H, NHC*H$_2$*C═O), 3.35 (s, 2 H, C*H$_2$*(C═O)$_2$), 3.04 (s, 3 H, NC*H$_3$*),

(35) Creighton, T. E. *Proteins: Structures and Molecular Principles*; Freeman: New York, 1984.

(36) (a) Joesten, M. D.; Schaad, L. J. *Hydrogen Bonding*; Marcel Dekker, Inc.: New York, 1974. (b) Pimentel, G. C.; McClellan, A. L. *The Hydrogen Bond*; Freeman: San Francisco, CA, 1960.

(37) Hamilton, W. C.; Ibers, J. A. *Hydrogen Bonding in Solids*; W. A. Benjamin, Inc.: New York, 1968.

2.96 (s, 3 H, NCH₃), 2.03 (br, 3 H, (CH)₃), 1.98 (br, 6 H, (CH₂)₃), 1.64 (br, 6 H, (CH₂)₃); ¹³C NMR (CDCl₃) δ 167.9, 167.5, 166.9, 52.1, 44.0, 41.4, 40.2, 37.6, 36.3, 35.7, 29.4; IR (0.001 M in CH₂Cl₂) 3439 (NH), 3416 (NH), 3317 (NH), 1690 (amide I), 1668 (amide I), 1640 (amide I), 1540 (amide II), 1515 (amide II) cm⁻¹; EI MS *m/e* 321.2056, calcd for C₁₇H₂₇N₃O₃ 321.2052. Anal. Calcd for C₁₇H₂₇N₃O₃: C, 63.53; H, 8.47; N, 13.07. Found: C, 63.79; H, 8.32; N, 13.09.

N-(tert-Butoxycarbonyl)-N-ethylglycine Methylamide. This material was prepared using the methodology of Cheung and Benoiton.[38] To a mixture of 3.2 g (80 mmol) of a 60 wt % sodium hydride dispersion in oil and 40 mL of THF at 0 °C was slowly added a solution of 3.5 g (20 mmol) of N-(tert-butoxycarbonyl)glycine and 6.5 mL (80 mmol) of iodoethane in 40 mL of THF. The reaction mixture was stirred under N₂ at 0 °C for 30 min and at room temperature for 96 h. The excess sodium hydride was neutralized by addition of 20 mL of MeOH and 20 mL of EtOAc. After evaporation of the solvent, the residue was partitioned between H₂O and EtOAc, and the organic layer was washed with 50% saturated aqueous NaHCO₃. The combined aqueous layers were acidified to pH = 3 with solid citric acid and extracted with several portions of EtOAc. The combined organic layers were washed with aqueous sodium thiosulfate, dried over MgSO₄, and evaporated to give 4.25 g (quantitative yield) of N-(tert-butoxycarbonyl)-N-ethylglycine as an orange oil: ¹H NMR (CDCl₃) 1:1 mixture of rotamers, δ 10.06 (br, 1 H, COOH), 3.98 and 3.89 (s, 2 H, NCH₂C=O), 3.4–3.3 (m, 2 H, NCH₂CH₃), 1.45 and 1.42 (s, 9 H, C(CH₃)₃), 1.10 (t, J = 7.2 Hz, 3 H, CH₃). This material was carried on without further purification.

To a solution of 2.03 g (10 mmol) of N-(tert-butoxycarbonyl)-N-ethylglycine in 75 mL of DMF was added 1.72 g (15 mmol) of N-hydroxysuccinimide, 2.57 g (12.5 mmol) of dicyclohexylcarbodiimide, 2.12 g (30 mmol) of methylamine hydrochloride, and 5 mL of triethylamine. A white precipitate quickly developed, and the mixture was stirred under N₂ for 24 h. The precipitate was removed by gravity filtration, and the filtrate was concentrated to a thick oil. Purification by SiO₂ column chromatography with 1–2% MeOH in CHCl₃ afforded 0.99 g (46% yield) of the desired amide as a thick, colorless oil: ¹H NMR (CDCl₃) δ 6.2 (br, 1 H, NH), 3.82 (s, 2 H, NCH₂C=O), 3.29 (q, J = 7.1 Hz, 2 H, NCH₂CH₃), 2.82 (d, J = 4.9 Hz, 3 H, NHCH₃), 1.46 (s, 9 H, C(CH₃)₃), 1.11 (t, J = 7.1 Hz, 3 H, CH₂CH₃); IR (CH₂Cl₂) 3445 (NH), 3373 (NH), 1696 (urethane C=O), 1679 (amide I), 1533 (amide II) cm⁻¹; EI MS *m/e* 202.1329, calcd for C₉H₁₃N₂O₃ 202.1317.

Triamide 7. To a solution of 0.1 g (0.6 mmol) of the mono-N,N-dimethylamide of malonic acid[7] in 5 mL of THF was added 0.11 g (1.0 mmol) of N-hydroxysuccinimide and 0.18 g (0.87 mmol) of dicyclohexylcarbodiimide; a white precipitate quickly developed. The mixture was stirred under N₂ for 1.5 h, and then a mixture of 0.2 mL (1.4 mmol) of triethylamine and N-ethylglycine methylamide hydrochloride (obtained from reaction of 0.13 g (0.6 mmol) of N-(tert-butoxycarbonyl)-N-ethylglycine methylamide with 5 mL of 4 N HCl in dioxane; dioxane was removed before subsequent reaction) in 15 mL of DMF was added. The resulting slurry was stirred under N₂ for 11 h, and the precipitate was then removed by gravity filtration. After concentration of the filtrate, the crude product was purified by SiO₂ column chromatography. The desired triamide was eluted with 4% MeOH in CHCl₃ as a colorless oil that slowly crystallized (0.11 g, 79% yield): mp 78–79.5 °C; ¹H NMR (CDCl₃) major rotamor (>92%), δ 7.89 (br, 1 H, NH), 4.09 (s, 2 H, NCH₂C=O), 3.53 (s, 2 H, CH₂(C=O)₂), 3.29 (q, J = 7.2 Hz, 2 H, NCH₂CH₃), 3.05 (s, 3 H, NCH₃), 3.01 (s, 3 H, NCH₃), 2.82 (d, J = 4.7 Hz, 3 H, NHCH₃), 1.20 (t, J = 7.2 Hz, 3 H, NCH₂CH₃); minor rotamer (<8%), δ 4.01 (s, 2 H, NCH₂C=O), 3.45 (q, J = 7.1 Hz, 2 H, NCH₂CH₃), 3.09 (s, 3 H, NCH₃), 2.98 (s, 3 H, NCH₃), 1.14 (t, J = 7.1 Hz, 3 H, NCH₂CH₃); ¹³C NMR (CDCl₃): δ 169.0, 168.3, 167.8, 49.1, 44.7, 40.4, 37.7, 35.7, 26.1, 14.1; IR (0.001 M in CH₂Cl₂) 3447 (NH), 3320 (NH), 1661 (amide I), 1638 (amide I), 1556 (amide II) cm⁻¹; EI MS *m/e* 229.1426, calcd for C₁₀H₁₉N₃O₃ 229.1413. Anal. Calcd for C₁₀H₁₉N₃O₃: C, 52.39; H, 8.35; N, 18.33. Found: C, 52.48; H, 8.31; N, 18.35.

Triamide 8. To a solution of 1.3 g (6 mmol) of N-(tert-butoxycarbonyl)-N-ethylalanine[39] in 45 mL of DMF was added 1.04 g (9 mmol) of N-hydroxysuccinimide, 1.55 g (7.5 mmol) of dicyclohexylcarbodiimide, 3 mL (21.5 mmol) of triethylamine, and 1.22 g (18 mmol) of methylamine hydrochloride. A white precipitate quickly developed, and the mixture was stirred under N₂ for 24 h. Solids were removed by gravity filtration, and the filtrate was concentrated to a thick oil. Purification by two

passes over a SiO₂ chromatography column eluting with 2% MeOH in CHCl₃ and with EtOAc afforded N-(tert-butoxycarbonyl)-N-ethylalanine methylamide as a colorless, viscous oil (0.65 g, 47% yield): ¹H NMR (CDCl₃) δ 6.1 (br, 1 H, NH), 4.5 (br, 1 H, NCHC=O), 3.4–3.0 (m, 2 H, NCH₂CH₃), 2.78 (d, J = 4.9 Hz, 3 H, NHCH₃), 1.46 (s, 9 H, C(CH₃)₃), 1.37 (d, J = 7.2 Hz, 3 H, CHCH₃), 1.11 (t, J = 7.0 Hz, 3 H, NCH₂CH₃). This material was carried on without further characterization.

Triamide **8** was prepared from the mono-N,N-dimethylamide of malonic acid and N-(tert-butoxycarbonyl)-N-ethylalanine methylamide by a procedure analogous to the preparation of triamide **7**. The crude product was purified by SiO₂ column chromatography eluting with 1–2% MeOH in CHCl₃ to afford triamide **8** as a white solid in a 49% yield: mp 88.5–89.5 °C; ¹H NMR (CDCl₃) major rotamer (~76%), δ 7.7 (br, 1 H, NH), 5.10 (q, J = 7.4 Hz, 1 H, NCHC=O), 3.52 (s, 2 H, CH₂-(C=O)₂), 3.5–3.1 (m, 1 H, NCH₂CH₃), 3.04 (s, 3 H, NCH₃), 2.99 (s, 3 H, NCH₃), 2.77 (d, J = 4.7 Hz, 3 H, NHCH₃), 1.48 (d, J = 7.4 Hz, 3 H, CHCH₃), 1.22 (t, J = 7.2 Hz, 3 H, NCH₂CH₃); minor rotamer (~24%), δ 7.8 (br, 1 H, NH), 4.43 (q, J = 6.9 Hz, 1 H, NCHC=O), 3.56 (s, 2 H, CH₂(C=O)₂), 3.13 (s, 3 H, NCH₃), 2.79 (d, J = 4.8 Hz, 3 H, NHCH₃), 1.36 (d, J = 7.0 Hz, 3 H, CHCH₃), 1.12 (t, J = 7.0 Hz, 3 H, NCH₂CH₃); ¹³C NMR (CD₂Cl₂) major rotamer, δ 171.7, 168.5, 168.2, 57.2, 41.6, 41.0, 37.8, 35.7, 26.4, 16.3, 14.9, minor rotamer, δ 170.8, 166.3, 40.9, 38.5, 38.1, 35.9, 26.3, 15.6, 14.0; IR (0.001 M in CH₂Cl₂) 3322 (NH), 1679 (amide I), 1650 (amide I), 1635 (amide I), 1550 (amide II) cm⁻¹; EI MS *m/e* 243.1583, calcd for C₁₁H₂₁N₃O₃ 243.1588. Anal. Calcd for C₁₁H₂₁N₃O₃: C, 54.30; H, 8.41; N, 17.27. Found: C, 54.39; H, 8.41; N, 16.96.

Triamide **11** was prepared from the mono-N,N-dimethylamide of malonic acid and N-(tert-butoxycarbonyl)glycine dimethylamide in a procedure analogous to that used for the preparation of triamide **7**. The crude product was purified by SiO₂ column chromatography eluting with 1–8% MeOH in CHCl₃ to afford the desired triamide as a white solid in 81% yield: mp 142.5–144 °C; ¹H NMR (CDCl₃) δ 8.21 (br, 1 H, NH), 4.07 (d, J = 4.3 Hz, 2 H, NHCH₂CO), 3.37 (s, 2 H, CH₂(C=O)₂), 3.05 (s, 3 H, NCH₃), 2.97 (s, 9 H, 3 NCH₃); ¹³C NMR (CDCl₃) δ 167.6, 167.5, 166.4, 41.4, 40.3, 37.7, 35.9, 35.6, 35.5; IR (0.001 M in CH₂Cl₂) 3440 (NH), 3394 (NH), 3290 (NH), 1671 (amide I), 1655 (amide I), 1634 (amide I), 1530 (amide II), 1499 (amide II) cm⁻¹; EI MS *m/e* 215.1269, calcd for C₉H₁₇N₃O₃ 215.1270. Anal. Calcd for C₉H₁₇-N₃O₃: C, 50.22; H, 7.96; N, 19.52. Found: C, 50.08; H, 7.79; N, 19.07.

Assignment of N–H Stretch Bands of Triamide 5 by H/D Exchange. The incorporation of deuterium into triamide **5** was monitored by ¹H NMR and FT-IR spectroscopies at room temperature. Experiments were carried out on a 10 mM solution of triamide **5** in 0.2 M CD₃OD in CDCl₃, which was prepared immediately before use. ¹H NMR spectra were recorded on a Bruker WP200 spectrometer. Chemical shifts were referenced to the signal for residual CHCl₃. Spectra were obtained after various time intervals as H/D exchange proceeded, and the extent of deuterium incorporation was judged by monitoring changes in the integrated areas of the amide proton signals. N–Hₐ (δ 7.70) was observed to exchange significantly faster than N–H_b (δ 6.77), and a concomitant loss of H–H coupling was observed for adjacent protons within the molecule. After 23 h of exchange, deuterium incorporation into N–Hₐ and N–H_b was approximately 85% and 45%, respectively.

FT-IR experiments were performed contemporaneously on the same solution used for ¹H NMR measurements. Spectra were obtained on a Nicolet 740 spectrometer, and solvent subtraction was carried out by using a reference spectrum obtained from a solution of 0.2 M CD₃OD in CDCl₃. Spectra (64 scans) were obtained every 10 min using a Nicolet kinetics program. Extent of deuterium incorporation was monitored by observing decreases in the absorbances of the non-hydrogen-bonded N–H stretching vibrations. The band at 3431 cm⁻¹ was observed to decrease in intensity much more rapidly than the band at 3453 cm⁻¹, allowing assignment of the former band as N–Hₐ, based on results of the ¹H NMR experiments.

Variable-Temperature NMR Experiments. Preparation of CD₂Cl₂ and CD₃CN solutions was performed as described previously.[7] CDCl₃ NMR samples (1 mM) were prepared from CDCl₃ stored over K₂CO₃ in a procedure analogous to that used for the preparation of CD₂Cl₂ samples, except that the solvent was not distilled. DMSO (10 mM) NMR samples were prepared without special precautions.

Variable-temperature NMR measurements were performed on a Bruker AM-500 spectrometer as described previously.[7] Nominal probe temperatures, read directly from the spectrometer console, were converted to actual temperatures by means of a calibration curve constructed with

(38) Cheung, S. T.; Benoiton, N. L. *Can. J. Chem.* **1976**, *55*, 906.
(39) Shuman, R. T.; Smithwick, E. L.; Smiley, D. L.; Brooke, G. S.; Gesellchen, P. D. *Peptides: Struct. Funct., Proc. Am. Pept. Symp.* Hruby, V. J.; Rich, D. H., **1983**, *8*, 143–6.

a chemical shift thermometer (0.03% concentrated HCl in MeOH).[40] To check the validity of this temperature correction, van't Hoff analyses were carried out on data obtained by this method and were compared to values obtained by measuring the NMR probe temperature with a chemical shift thermometer before and after each sample analysis. $\Delta H°$ values varied by at most 0.1 kcal/mol, and $\Delta S°$ values varied by at most 0.4 eu, indicating that the use of a temperature calibration curve introduces little or no error into these van't Hoff analyses.

Variable-temperature IR experiments were carried out on a Nicolet 740 spectrometer as previously described.[7] For amides examined in CH_2Cl_2, aggregation was ruled out by comparing N–H stretch and amide I spectra at 1.0 and 0.25 mM: aggregation was ruled out if subtraction, with an appropriate multiplication factor, produced a flat base line. DMSO solutions were prepared with solvent that had been stored over 4-Å molecular sieves. Base line corrections were employed to eliminate base line tilt and to bring background absorbance to 0. However, no base line corrections were applied to eliminate base line curvature. For quantitative analyses, integration of N–H stretching absorbance was performed over a moving window of $\nu_{max} \pm 25$ cm^{-1}.

IR Experiments with Added D_2O. At 298 K, the solubility of water in CH_2Cl_2 is approximately 150 mM; this solubility drops to roughly 60 mM at 273 K and 10 mM at 243 K.[41] Variable-temperature IR studies with CH_2Cl_2 containing more than trace (5–10 mM) concentrations of water are hampered by two problems: at higher temperatures tailing from the intense O–H stretch absorptions (3500–3600 cm^{-1}) obscures the N–H stretch bands, and at lower temperatures the water frozen out on the IR cell window obscures the sample. In order to overcome the former problem, we used D_2O, and in order to minimize the latter problem, we restricted our studies to the range 255–297 K (three temperatures). We compared solutions containing 1 mM 3 that were 10% or 20% saturated with D_2O (i.e., approximately 15 or 30 mM D_2O) with a "dry" solution.[42] Methylene chloride solutions of diamide 3 (1 mM) with varying percentages of D_2O saturation were prepared by dilution of 10 mM diamide in "dry" CH_2Cl_2 with appropriate proportions of dry solvent and D_2O-saturated solvent, the latter prepared by shaking D_2O and CH_2Cl_2 in a separatory funnel and separating the layers. Three-point van't Hoff plots were constructed for these three different water concentrations. The deduced enthalpy and entropy of hydrogen-bonded ring formation were not significantly affected by the varying concentration of D_2O among these samples (0 mM added D_2O, $\Delta H° = +0.29$ kcal/mol, $\Delta S° = +1.0$ eu; 15 mM added D_2O, $\Delta H° = +0.31$ kcal/mol, $\Delta S° = +1.0$ eu; 30 mM added D_2O, $\Delta H° = +0.30$ kcal/mol, $\Delta S° = +1.1$ eu. For these experiments, dry solvent backgrounds were used for all solvent subtractions.

Curve Fitting of FT-IR Spectral Data. van't Hoff analysis of hydrogen-bond formation within triamide 5, based on FT-IR measurements, is described in the text. Because of band overlap in the N–H stretching region of this compound, curve-fitting procedures were required to determine integrated areas of non-hydrogen-bonded N–H$_b$. These procedures were carried out using the Nicolet FOCAS™ software package. For triamide 5, only the region from 3500–3180 cm^{-1} was subjected to curve analysis. The spectra were base line corrected to adjust the absorbances at 3500 cm^{-1} and 3180 cm^{-1} to 0. No base line correction to adjust base line curvature was employed.

The first step in the curve-fitting procedure involved Fourier self-deconvolution of the base line-corrected spectral data. This method provides resolution enhancement of the data and allows assignment of

peak positions. Because non-hydrogen-bonded N–H bands are generally much narrower than hydrogen-bonded N–H bands, the self-deconvolution was performed in two steps. First, the non-hydrogen-bonded N–H bands were deconvoluted using a width at half maximum of 25 cm^{-1}, a width-deflation factor of 2.20, and a Sinc squared apodization function. Two non-hydrogen-bonded N–H bands were assigned in each spectrum. Second, the hydrogen-bonded N–H bands were deconvoluted using a width at half maximum of 50 cm^{-1}, a width-deflation factor of 1.5, and a Sinc squared apodization function. Two hydrogen-bonded bands were assigned in each spectrum.

After assigning approximate peak positions, curve-fitting optimization was employed. Four variables were adjusted for each peak: peak position, peak intensity, width at half maximum, and percent Gaussian vs Lorentzian. These variables were adjusted manually until the calculated spectrum qualitatively fit the original spectral data. The program was then allowed to optimize these parameters to give the best fit to the original data. It was found that if the optimization was repeated, starting with parameter values obtained from the computer optimization, new values for these parameters were often obtained. Therefore, the optimization was repeated from the ending point of the preceding optimization until the same values for all variables were obtained three consecutive times.

Once the curve-fitting had been optimized, the area of the calculated free N–H$_b$ band was determined by integration over a moving window of $\nu_{max} \pm 50$ cm^{-1}. Extinction coefficients for this band were estimated using spectral data obtained for lactic acid derivative 14. These spectra were subjected to curve fitting by a similar procedure, employing a window of $\nu_{max} \pm 50$ cm^{-1}. Fourier self-deconvolution employed a full width at half maximum of 25 cm^{-1}, a width deflation factor of 2.2, and an Sinc squared apodization function. In all cases, these spectra were fit to a single calculated band.

The curve fitting analyses were carried out over three sets of variable-temperature FT-IR data for triamide 5 and three sets of data for ester amide 14. van't Hoff calculations were performed on all nine combinations of spectral data. In general, excellent agreement was obtained between trials of triamide 5, but rather poor reproducibility was observed for ester amide 14 data, resulting in significant scatter in the calculated thermodynamic parameters for triamide 5.

Note Added in Proof: McDonald and Still have recently shown that reparametrization of AMBER, based on the results of high-level ab initio calculations for small amide molecules, leads to a force field (AMBER*) that successfully predicts 1c to be the most enthalpically favorable folding pattern of 1 in chloroform solution (McDonald, D. Q.; Still, W. C. *Tetrahedron Lett.* **1992**, *33*, 7743, 7747).

(40) Van Geet, A. L. *Anal. Chem.* **1970**, *42*, 679.

(41) *Ullman's Encyclopedia of Industrial Chemistry*; VCH Verlagsgesellschaft: Weinheim, 1985; Vol. A6, pp 237–238.

(42) The effects of H/D exchange of the amide proton were not detectable in freshly prepared "wet" samples; such exchange was, however, observed over the course of several hours in fully D_2O-saturated solutions.